

## **Author's response**

### **Response to gmd-2020-59-RC1**

Dear Dr. Astrid Kerckweg

Thank you for your comments on python script DOI and the datasets in our paper.

According to your comments, I have published the python code at GitHub and Zenodo.

The data also has been described clearly in GitHub README.md. The results in this paper could be reproduced by using data in GitHub.

Please check the following link of the python script:

Link: <https://zenodo.org/record/3937226#.Xw2M6egzZPY>

DOI: 10.5281/zenodo.3937226

I have given the specification in the manuscript, please check the attached file.

Please check line 284-285, 560-563

Thanks again for your professional comments!

Any question please contact me.

Kind regards

Batu

## Response to gmd-2020-59-RC2

This manuscript tests whether XGBoost can provide alternative insights that conventional land-use models are unable to generate. The overall methodology is interesting. I have a number of major comments before I can suggest the paper for publication.

We appreciate the thoroughness with which you went through our manuscript. We consider all your comments as very useful, even though we may have disagreed here and there. We believe that with the help of your work, this manuscript has further improved. Thank you!

1, Line 54: “Some such models are spatial (e.g. CLUE-S, GeoSOS-FLUS, LTM, Fu et al., 2018; Liang et al., 2018; Pijanowski et al., 2002, 2005; Verburg & Veldkamp, 2004; Zhang et al., 2013); others are not (e.g. Markov models; Iacono et al., 2015; Yuan et al., 2015).” Authors should be aware that all land use change models are spatial models. Markov models are used to estimate the quantity of change from one land use state to another but are not land use change simulators.

**Response:** Thank you for your interesting discussion. In fact, we were to say that some models are spatially explicit, and some are not. We have corrected this in line 55-56. Markov models are not spatially explicit and can deal with numbers without any spatial relation. However, we agree with you that of course all land-use models refer to a spatial concept.

2, Line 57: “Hybrid models, which combine different approaches to make the best use of the advantages of each model, are another important variety. This type of model is used to characterize the multiple aspects of LUCC patterns and processes (Li and Yeh, 2002; Sun and Müller, 2013).” Authors did not discuss important other land use modeling approaches such as Cellular Automata (CA), Agent-Based (AB) and a hybrid CA-AB (e.g., Mustafa et al., 2018, 2017; Vermeiren et al., 2016).

**Response:** We have added a discussion about these models as you suggested in line 56-66.

3, Line 143: “The DEM data were extracted from the SRTM 90m resolution and, after resampling, all data were processed into 1×1 km<sup>2</sup> raster files.” Why do you resample the data to such low resolution? and what is the resample method do you employ?

Response: A total of twenty drivers was used in this paper. Two of them, population density and GDP density, were at 1×1 km<sup>2</sup>, two other, temperature and precipitation, were at even coarser resolution (station-based). 1×1 km<sup>2</sup> seemed a good compromise between the finest and the coarsest resolution. In addition, the area of study region is 20.4×10<sup>4</sup> km<sup>2</sup>, for which a finer resolution would not have seemed appropriate. We resampled by using the NEAREST method in ArcGIS. We have added this in the manuscript at line 150.

4, Line 146: “All distance measures were extracted from LUCC datasets from the years 2000 and 2015 using ArcGIS Euclidean distance”. Euclidean distance is a basic GIS process that can be performed by many tools. No need to mention specific software for such a basic GIS analysis. -Table 1 presents data with inconsistent dates (2000, 2015, or 2000, 2010). Please justify as this will bias the results.

Response: With respect to reproducibility, we remain with giving the tool for computing the Euclidian distance. High-resolution population and GDP density were only available for 2000 and 2010. We have added a discussion on the bias that could be caused by this data. Please check line 160-164.

5, Line 207: “In our case study, 18,190 pixels (about 10% of the total) were selected by different sampling methods (Fig. S 3) to train (66% of the sample size) and test (34% of the sample size) the model.” Please provide more details about your sample. Is it a binary (0 no changes, 1 changes) excluding grassland with no change between 1975 and 2015?

Response: As you suggested, we have added a more detailed description of the sample in line 216-221.

6, Figures 3 and 4: this evaluation of model performance was done for which period 1975-2000 or 2000-2015? AND do you consider all cells in the study are or the observed changes between two dates? Also, there is a sharp difference in performance between the Logit model and XGB, why? According to many studies that compared Logit with machine learning (ML) methods, ML outperformed logit but not such huge differences as presented in this study.

Response: Thank you for your detailed question.

1) The model performance was done for the newly added grassland in both periods

2) We are not surprised by this large difference. The tree-based models are always expected to outperform linear models. We have used 33% of the data for validation, which were not included in the training. So, over-training should not be an issue, so we have to assume that the difference between the linear and non-linear approach is responsible for this difference in performance.

7, Figure 6: can you present the variables' importance (Odds ratio) of the logit model as well? This will help readers to understand the differences between the two methods.

Response: As you mentioned, SHAP values as a statistical method could be combined with many other ML models to present the variables' importance. However, the Logistic regression model is not a robust model in simulating grassland degradation in this study. The kappa index is 0.72. To present variables' importance using such a weak model does not make any sense to us. The Logistic regression was used as benchmark in this study and has proven that a non-linear machine learning model could achieve a better predictive quality than linear methods. This is the aim of this study. We have put it down here for you, but we think that it is not providing any additional information for the reader. For this reason, we refrain from adding it to the manuscript.

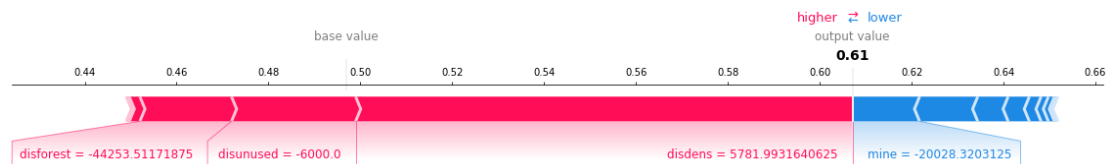


Figure 1: Decomposed SHAP values for the individual prediction of an example pixel (Logistic regression model).

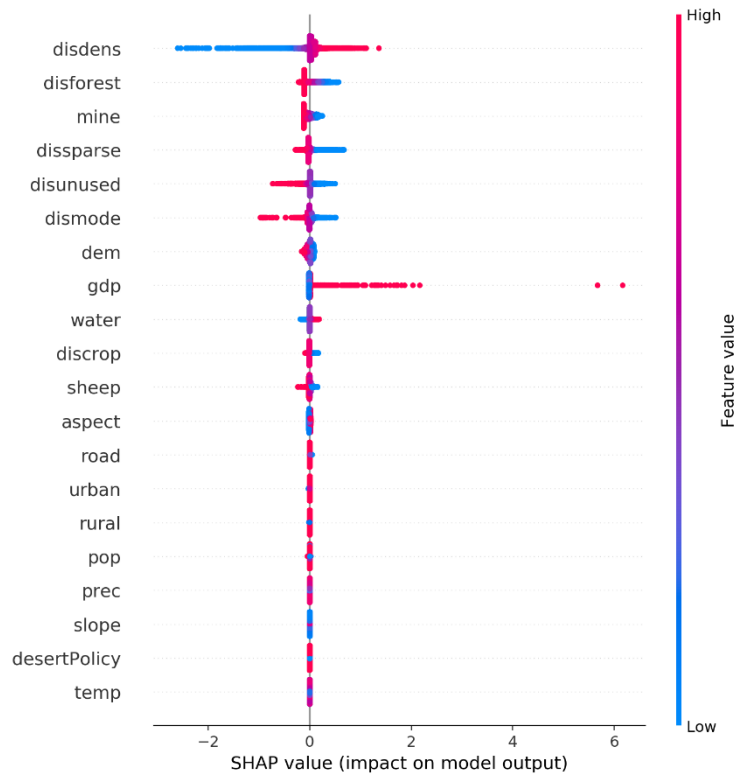
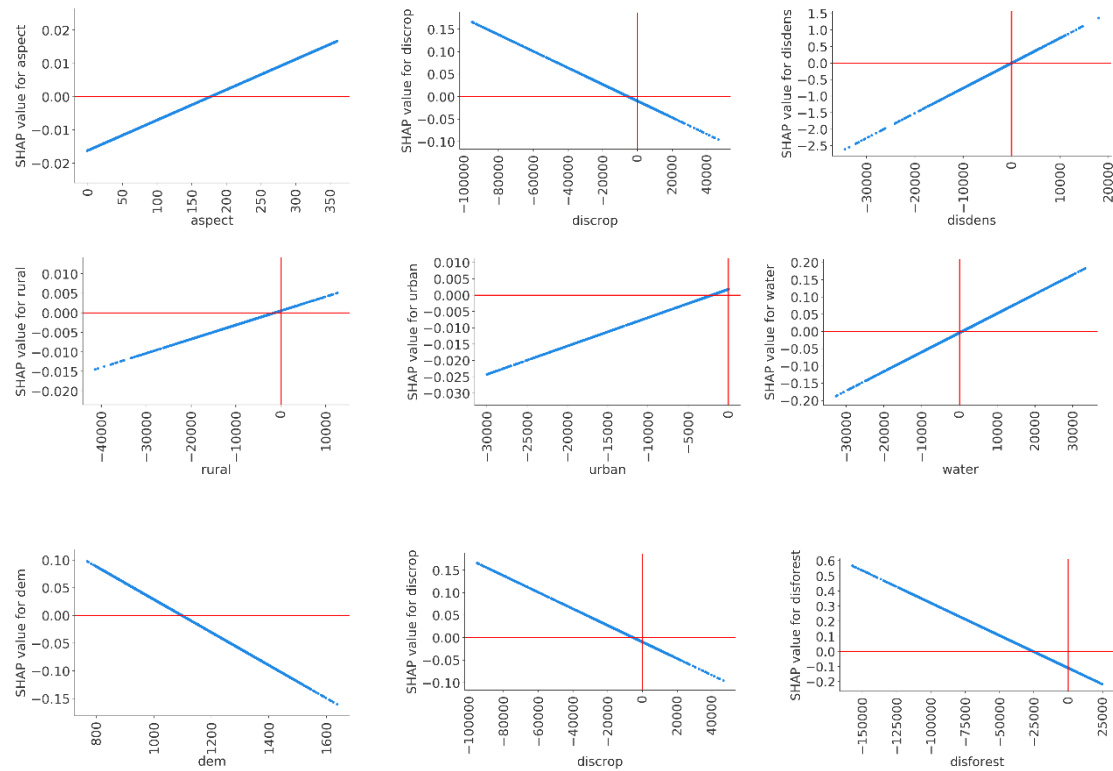


Figure 2: Driver ranking by SHAP values based on the training dataset (66% of sample size) using the over-sampling method (Logistic regression model).



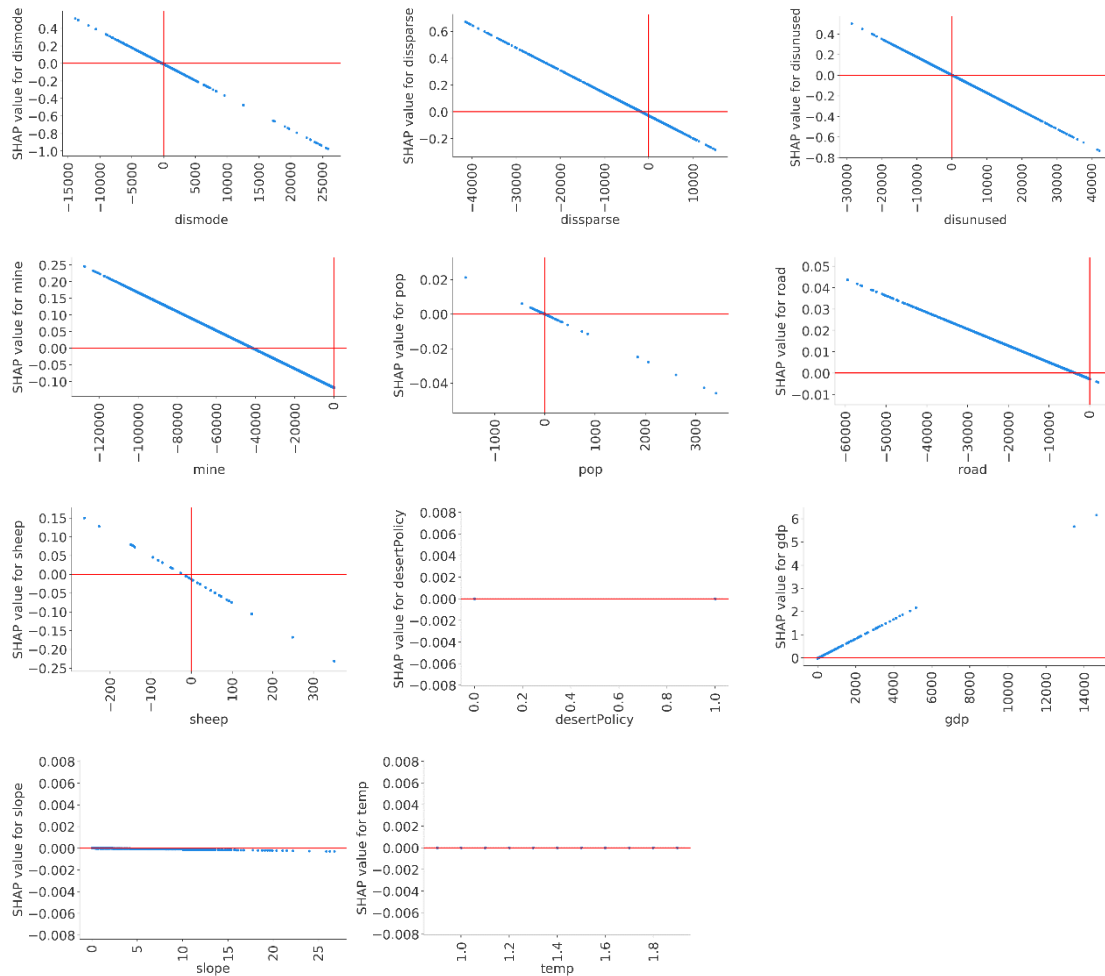


Figure 3: The SHAP dependence plot for each driver (Logistic regression model).

8, Figure 9: I am confused about this probability map. I see that almost all pixels have a probability of either 100% (1) or 0% (0). So, is it really a gradient probability map?

It is, but in fact, the number of pixels that have values between 0 and 100 is small. On top, we have 86% of the pixels defined as grassland, which is why the map looks almost complete, but it is not. We have adjusted the map and included a zoom in to one region where more gradient values are located, please check in line 428-430

Another fundamental question, if we need to simulate future scenarios that assume a change of 100 pixels out of 1000 pixels (as an example) then this map is not useful as many pixels have a probability value of 100%. Should the model make a random selection from pixels with a 100% probability??

You are right, for prediction purposes this map is not useful. We have already discussed the difficulties that occur if you used such approach to simulate future or other hypothetical scenarios and concluded that the ML approach must be combined with other modelling approaches in order to be able to produce scenarios. In this case, we just demonstrate with this map the vulnerability of the region to further grassland degradation. The probability for grassland degradation is the closest we can get to a spatial explicit prediction using XGBoost and SHAP.

9, English needs improvements.

This manuscript has been reviewed by a professional British language editor for scientific publications.

## Response to gmd-2020-59-RC3

1

2 1, Thank you for your interesting submission. This paper presents an interesting suite  
3 of tools for investigating an important topic of research. I have only some minor  
4 comments to make before publication:

5 **Response: We appreciate your suggestions for our manuscript and we consider all your**  
6 **comments as very useful. We have addressed each of your comments below.**

7

8 2, As with any ML interpretation, one wonders how more generally useful this is to  
9 other regions. Have you considered whether testing against historical datasets is  
10 worthwhile?

11 In other words, have you tried to apply this method to re-analyses previously studied  
12 grassland degradation? If not, are there similar areas of focus this might work on?

13 **Response: Thank you for your useful question.**

14 **We have not yet been able to test this method in another region or to historical datasets.**

15 **But the method in this study has certainly the potential for transferability for two**  
16 **reasons:**

17 **First of all, we have used this method on another topic and dataset in the same region,**  
18 **namely for studying land degradation. Please see Land-use change and land degradation**  
19 **on the Mongolian Plateau from 1975 to 2015 — a case study from Xilingol, China.**  
20 **Land Degradation & Development 29: 1595–1606. DOI: 10.1002/ldr.2948. XGBoost**  
21 **and SHAP presented an excellent performance as well.**

22 **Secondly, the datasets in this study (land use and driver data) are public and available**  
23 **and could be replaced by other datasets. For more information please see the data**  
24 **description in the manuscript, line 171-173.**

25 **Based on this, we believe XGBoost and SHAP provide large potential to be applied to**  
26 **other datasets, regions and topics as well.**

27 **Actually, the datasets in this manuscript are historical data and we predict the dynamic**  
28 **grassland degradation (newly added grassland degradation, NGD) between 2000-2015**  
29 **in Xilingol based on historical data from 1975 to 2015. Then we use the historical data**  
30 **from 2000-2015 to test the predicted NGD between 2000-2015. The results indicated**  
31 **that it is worthwhile testing against the historical data.**

32 **More detailed information about the data in this manuscript please check line 143-170.**  
33 **In addition, for a ML model,**

34



35 3, Please can you comment on the computer hardware required for training?

36 Response: Done.

37 I comment the computer hardware in “Code and data availability” section, please check  
38 line 582-594.

39 The used XGBoost algorithm including the SHAP library runs well on a modern (Intel  
40 or AMD) PC (4 cores or more, 16 GB RAM). The training and the simulation were  
41 made on Linux as operating system but should work also under Windows.

42

43 4, Please include a Zenodo, or other archive, snapshot of the data used in this study.  
44 Thanks!

45 Response: Thank you for your careful comments, I have published the python code at  
46 GitHub and Zenodo. The data also has been described clearly in GitHub README.md.  
47 The results in this paper could be reproduced by using data in GitHub.

48 Please check the following link of the python script:

49 Link: <https://zenodo.org/record/3937226#.Xw2M6egzZPY>

50 DOI: 10.5281/zenodo.3937226

51 I have given the specification in the manuscript, please check the attached file.

52 Please check line 284-285, 560-563

53

54

55 **Using SHAP to interpret XGBoost predictions of grassland**  
56 **degradation in Xilingol, China**

57 Batunacun<sup>1,2\*</sup>, Ralf Wieland<sup>2</sup>, Tobia Lakes<sup>1,3</sup>, Claas Nendel<sup>2,3</sup>

58 <sup>1</sup> Department of Geography, Humboldt-Universität zu Berlin, Unter den Linden 6, 10099 Berlin, Germany

59 <sup>2</sup> Leibniz Centre for Agricultural Landscape Research (ZALF), Eberswalder Straße 84, 15374, Müncheberg, Germany

60 <sup>3</sup> Integrative Research Institute on Transformations of Human-Environment Systems, Humboldt-Universität zu Berlin, Friedrichstraße  
61 191, 10099 Berlin, Germany

---

\* Correspondence to: Institute of Landscape Systems Analysis, Leibniz Centre for Agricultural Landscape Research (ZALF), Eberswalder Straße 84, 15374, Müncheberg, Germany

E-mail: batunacun@zalf.de

## 62 Abstract

63 Machine learning (ML) and data-driven approaches are increasingly used in many research areas.  
64 XGBoost is a tree boosting method that has evolved into a state-of-the-art approach for many ML  
65 challenges. However, it has rarely been used in simulations of land use change so far. Xilingol, a  
66 typical region for research on serious grassland degradation and its drivers, was selected as a case  
67 study to test whether XGBoost can provide alternative insights that conventional land-use models  
68 are unable to generate. A set of twenty drivers was analysed using XGBoost, involving four  
69 alternative sampling strategies, and SHAP to interpret the results of the purely data-driven approach.  
70 The results indicated that, with three of the sampling strategies (over-balanced, balanced and  
71 imbalanced), XGBoost achieved similar and robust simulation results. SHAP values were useful for  
72 analysing the complex relationship between the different drivers of grassland degradation. Four  
73 drivers accounted for 99% of the grassland degradation dynamics in Xilingol. These four drivers  
74 were spatially allocated, and a risk map of further degradation was produced. The limitations of  
75 using XGBoost to predict future land-use change are discussed.

76 **Key words:** grassland degradation, machine learning, driver-driven method, XGBoost, SHAP  
77 values

## 78 1. Introduction

79 Land-use and land-cover change (LUCC) has received increasing attention in recent years (Aburas  
80 et al., 2019; Diouf & Lambin, 2001; Lambin et al., 2003; Verburg et al., 2002). Land-use change  
81 includes various land-use processes, such as urbanisation, land degradation, water body shrinkage,  
82 and surface mining, and has significant effects on ecosystem services and functions (Sohl &  
83 Benjamin, 2012). Grassland is the major land-use type on the Mongolian Plateau; its degradation  
84 was first witnessed in the 1960s. About 15% of the total grassland area was characterised as being  
85 degraded in the 1970s, which rose to 50% in the mid-1980s (Kwon et al., 2016). In general,  
86 grassland degradation (GD) refers to any biotic disturbance in which grass struggles to grow or can  
87 no longer exist due to physical stress (e.g. overgrazing, trampling) or changes in growing conditions  
88 (e.g. climate; Akiyama & Kawamura, 2007). In this study, grassland degradation is defined as  
89 grassland that has been destroyed and subsequently classified as some other land use, or that has  
90 significantly decreased in coverage.

91 Grassland is a land use that provides extensive ecosystem services (Bengtsson et al., 2019). When  
92 degraded, the consequences are seen in an immediate decline in these services, such as a decrease  
93 in carbon storage due to a reduction in vegetation productivity (Li et al., 2017). About 90% of carbon  
94 in grassland ecosystems is stored in the soil (Nkonya et al., 2016). Furthermore, GD results in a  
95 reduction in plant diversity and above-ground biomass available for grazing (Wang et al., 2014).  
96 Likewise, GD leads to soil erosion and frequent dust storms in Inner Mongolia (Hoffmann et al.,  
97 2008; Reiche, 2014). Drivers of GD are manifold, and have been analysed in a range of studies ([Li  
98 et al., 2012](#); [Liu et al., 2019](#); [Sun et al., 2017](#); [Xie and Sha, 2012](#))([Li et al., 2012](#); [Liu et al., 2019](#);  
99 [Sun et al., 2017](#); [Xie and Sha, 2012](#)). However, few studies use sophisticated driver analysis to  
100 predict spatial patterns of GD (Jacquin et al., 2016; Wang et al., 2018). A number of studies have  
101 addressed the complex relationship between GD and its drivers ([Cao et al., 2013a](#); [Feng et al., 2011](#);  
102 [Fu et al., 2018](#); [Tiscornia et al., 2019a](#))([Cao et al., 2013a](#); [Feng et al., 2011](#); [Fu et al., 2018](#); [Tiscornia  
103 et al., 2019a](#)). However, these studies focus mainly on visualising or describing non-linear  
104 relationships between GD and its drivers.

105 The aim of developing various land-use models was to explore the causes and outcomes of land-use  
106 dynamics; these models were implemented in combination with scenario analysis to support land

107 management and decision-making (National Research Council, 2014; Ren et al., 2019). Most such  
108 models are statistical models, such as logistic regression models or models based on principle  
109 component analysis (Li et al., 2013; Lin et al., 2014) or Bayesian belief networks (Krüger and Lakes,  
110 2015). Some such models are ~~spatial~~spatially explicit (e.g. CLUE-S, GeoSOS-FLUS, LTM, Fu *et*  
111 *al.*, 2018; Liang *et al.*, 2018; Pijanowski *et al.*, 2002, 2005; Verburg & Veldkamp, 2004; Zhang *et*  
112 *al.*, 2013); others are not (e.g. Markov models; Iacono et al., 2015; Yuan et al., 2015). Hybrid models,  
113 which combine different approaches to make the best use of the advantages of each model, are  
114 another important variety. This type of model is used to characterise the multiple aspects of LUCC  
115 patterns and processes (Li and Yeh, 2002; Sun and Müller, 2013). Agent-based models (ABM)  
116 simulate land use change decisions based on the behaviour of individual decision-makers. They  
117 often consider economic and political information to calculate land-use change. Cellular Automata  
118 (CA) models are gridded models in which time, space, and state are all discrete. CA models are  
119 spatially explicit and land use change decisions are made based on the state of the neighbouring  
120 cells (Yang et al., 2014). CA models are often used for the spatial allocation of land use and land  
121 cover at a high spatial resolution (Cao et al., 2019) and may be used in combination with other  
122 models, such as ABM (e.g., Charif et al., 2017; Mustafa et al., 2017; Troost et al., 2015; Vermeiren  
123 et al., 2016).

124 In most cases of land-use change, it was either assumed that the relationship between the drivers  
125 and the resulting land-use change is constant over time (Fu et al., 2018; Samie et al., 2017; Zhan J  
126 Y et al., 2007), or the relationships were identified as being linear or non-linear, but were not  
127 interpreted (Tayyebi and Pijanowski, 2014a). We hypothesise that the relationships between GD and  
128 its drivers are mainly non-linear. We therefore see a need for methods that are capable of analysing  
129 and interpreting non-linear relationships between GD and dynamic drivers.

130 With the development of computer science, machine learning (ML) models have been increasingly  
131 used in land-use change modelling (Islam et al., 2018; Krüger and Lakes, 2015; Lakes et al., 2009;  
132 Tayyebi and Pijanowski, 2014a). ML is superior to the human brain when it comes to pattern  
133 recognition in large datasets, e.g. images and sensor fields. Once the task is defined and the data for  
134 training is provided, ML operates without any further human assistance. Various ML approaches  
135 have been used in the analysis of land-use change processes, the most prominent of which being  
136 Support Vector Machines (SVM, Huang *et al.*, 2009, 2010), Artificial Neural Networks (ANN,  
137 Ahmadlou *et al.*, 2016; Yang *et al.*, 2016), Classification And Regression Trees (Tayyebi and  
138 Pijanowski, 2014b) and Random Forest (RF, Freeman *et al.*, 2016). While the different ML  
139 approaches generally perform well in identifying patterns, they remain a black box and make no  
140 contribution to our understanding of how the underlying drivers act on the LUCC process.  
141 Compared to linear methods such as logistic regression, ML models often achieve higher accuracy  
142 and capture non-linear land-use change processes. Likewise, ML models relax some of the rigorous  
143 assumptions inherent in conventional models, but at the expense of an unknown contribution of  
144 parameters to the outcomes (Lakes et al., 2009). However, the key challenge is to crack the black  
145 box and reveal how each driver affects the land-use change pattern or processes in the ML models.

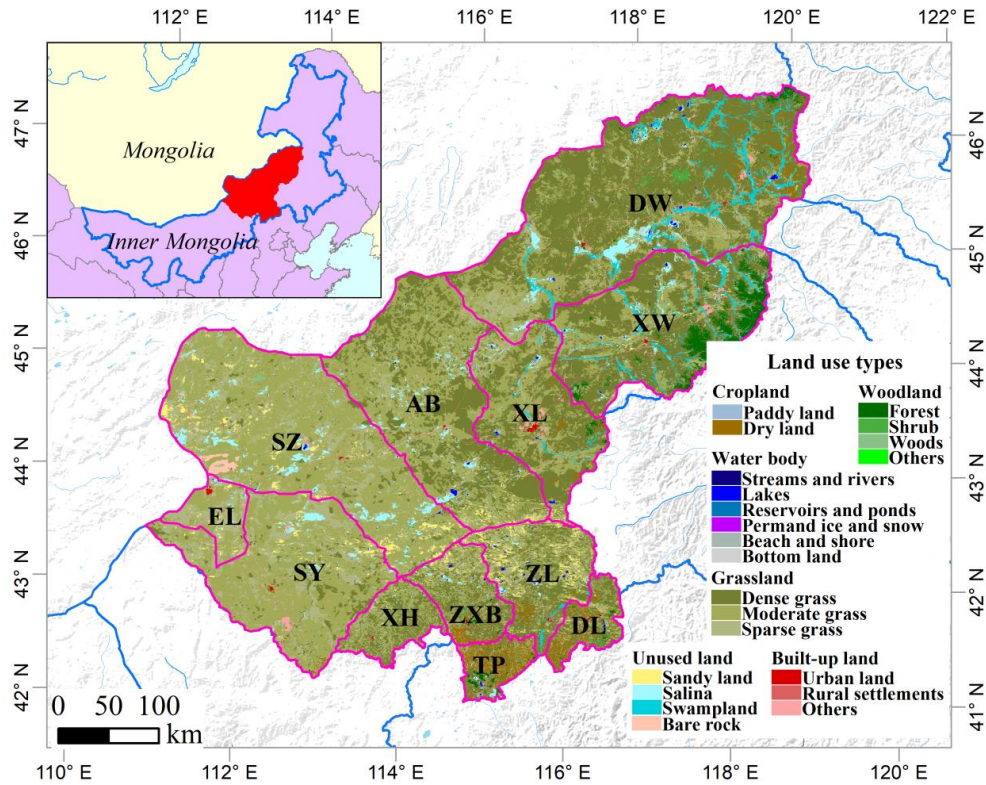
146 The eXtreme Gradient Boosting (XGBoost) method has recently been developed as a supervised  
147 machine learning approach (Chen and Guestrin, 2016). XGBoost algorithms have achieved superior  
148 results in many ML challenges; they are characterised by being ten times faster than popular existing  
149 solutions, and the ability to handle sparse datasets and to process hundreds of millions of examples.  
150 XGBoost has already been used in land-use change detection, combined with remote sensing data  
151 (Georganos et al., 2018), but has not yet been used in the simulation and prediction of land-use  
152 change. SHapley Additive exPlanations (SHAP; Lundberg & Lee, 2016) is a unified approach to  
153 explain the output of any ML model and to visualise and describe the complex causal relationship  
154 between driving forces and the prediction target. We propose using SHAP to analyse the driver  
155 relationships hidden in the black box model of XGBoost when employed for land-use change  
156 modelling.

157 Having earlier used a clustering approach to identify drivers of GD in a case study in Inner Mongolia  
158 (Xilingol League; Batunacun *et al.*, 2019), we now use XGBoost and SHAP to simulate GD  
159 dynamics across the same area. We are primarily interested in learning whether ML models can  
160 achieve a better predictive quality than linear methods, in addition to improving our understanding  
161 of how grassland degrades in Xilingol. In the intention to identify areas with a high risk of further  
162 degradation and to determine the drivers responsible for progressive degradation, we used XGBoost  
163 to generate a data-driven model to explore the GD patterns. We then used SHAP to open the non-  
164 linear relationships of the black box model stepwise, and transformed these relationships into  
165 interpretable rules. The resulting model enabled us to map the primary GD drivers and GD hot spots  
166 in Xilingol.

## 167 **2. Materials and Methods**

### 168 **2.1 Study area**

169 The Xilingol League is located about 600 km north of Beijing (He *et al.*, 2004), in the centre of  
170 Inner Mongolia. This administrative unit, covering an area of 206,000 km<sup>2</sup>, spans from 41.4°N to  
171 46.6°N and from 111.1°E to 119.7°E (Figure 1). The area is dominated by the continental temperate  
172 semiarid climate. The frequent droughts (in summer) and “dzud” (an extremely harsh and snow-  
173 rich winter) are the major natural disasters that occasionally lead to catastrophic livestock losses in  
174 this region (Allington *et al.*, 2018; Tong *et al.*, 2017; Xu GC *et al.*, 2014). Xilingol possessed about  
175 18,104 km<sup>2</sup> available pasture resources and 1240.4·10<sup>4</sup> sheep units at the end of 2015 (Xie and Sha,  
176 2012). Around 1.044 million people lived in Xilingol in 2015, with ethnic Mongolian minorities  
177 accounting for around 31% and the rural population for 37% (~~Batunacun *et al.*, 2019; Shao *et al.*,  
178 2017~~)(Batunacun *et al.*, 2019; Shao *et al.*, 2017). Xilingol is a vast grassland, known for its high-  
179 quality meat products, nomadic culture, rich mineral resources and ethnic minorities. The ongoing  
180 degradation of grassland is receiving increasing attention. A set of economic stimuli and ecological  
181 protection policies launched in Xilingol were viewed as the root cause of GD over the past four  
182 decades. Although large-scale ecological restoration policies were implemented after 2000 in a bid  
183 to reduce GD, the problem still persists.



184

185 Figure 1: The location of the Xilingol League in Inner Mongolia and its land uses.

186 **2.2 Grassland degradation**

187 This study defines grassland degradation (GD) based on land-use conversion, involving two kinds  
 188 of land-use change processes: (i) the complete destruction of grassland by transformation to another  
 189 type of land use (built-up land, cropland, woodland, water bodies and unused land), and (ii) a decline  
 190 in grassland coverage, which includes dense grass deteriorating into moderately dense grass and  
 191 sparse grass, and moderately dense grass deteriorating into sparse grass (see Fig. S 1a). Given that  
 192 GD is a dynamic process, we intended in this study to find the major drivers of newly added  
 193 grassland degradation (NGD). NGD refers to the difference in spatial GD extent between two  
 194 periods. About 13.0% of the total grassland area (176,410 km<sup>2</sup> in 2015) was degraded between 1975  
 195 and 2000 (Fig. S 1b); a further 10.6% was degraded in 2000-2015 (Fig. S 1c). Comparing the two  
 196 periods, approximately 10.2% of the grassland corresponded to the NGD area across the whole  
 197 region (Fig. S 1d). 18,093 pixels were extracted from the total NGD area, while the pixel number  
 198 of conversion for other land uses is 178,990 in this study (hereafter: non-NGD).

199 **2.3 Data collection**

200 In line with previous studies, a checklist of possible drivers (D) of GD was developed from the literature  
 201 (Cao et al., 2013b; Sun et al., 2017). A total of 19 drivers were grouped into four categories (see Table  
 202 1). All categories were described as follows: (1) Climate factors, including the annual mean temperature  
 203 (T) and annual sum of precipitation (P) in the growing season (April to Sep), were extracted from the  
 204 longest available weather dataset (from 1958-2015), in combination with evaluation data and the kriging  
 205 algorithm, to produce 1×1 km<sup>2</sup> raster files. (2) Geographic factors include elevation (DEM), and slope  
 206 and aspect (extracted from DEM data), which can be treated as the characteristic of each grid cell. The  
 207 DEM data were extracted from the SRTM 90m resolution and, after resampling [using the NEAREST](#)

208 method in ArcGIS, all data were processed into 1×1 km<sup>2</sup> raster files. (3) Distance measures (the distance  
209 of each pixel centre to urban, rural, road and mining, forest, cropland, dense grass, moderately dense  
210 grass, sparse grass and unused land pixels) are widely used factors for different land-use models (Khoury,  
211 2012; Samardžić-Petrović et al., 2016, 2017; Zhang et al., 2013). All distance measures were extracted  
212 from LUCC datasets from the years 2000 and 2015 using ArcGIS Euclidean distance, and processed into  
213 1×1 km<sup>2</sup> grids. (4) Socio-economic factors include the gross domestic product (GDP), ~~sheep density~~  
214 and population density from 2000 and 2010, and sheep density from 2000 and 2015. GDP and population  
215 density were obtained from a resources and environment data cloud platform, CAS  
216 (<http://www.resdc.cn/>); sheep density data were accessed from statistical data; and we converted all  
217 livestock data into grassland pixels. Unfortunately, high-resolution GDP and population density data was  
218 not available for 2015 to match the other data that was recorded for that year, so we may assume that  
219 GDP and population density introduce a bias to the result. While population density did not change much  
220 between 2010 and 2015, GDP changed from 61.4 billion Yuan in 2010 to 100.2 billion Yuan in 2015 in  
221 total over the Xilingol region (GDP data source: <http://tjj.xlgl.gov.cn/ywlm/tjsj/jdsj/>). (5) Finally, we  
222 identified an area in which we assumed a strong policy impact in the past, and developed a proxy for the  
223 policy effect on grassland degradation. Here, a range of ecological protection measures were  
224 implemented inside and outside the Hunshandake and Wuzhumuqin sand lands (see Fig. S 2), e.g. a  
225 livestock ban and the promotion of chicken farming (Su et al., 2015). In a bid to explore policy effects,  
226 we assumed that GD is effectively slowed down by various policies inside the sandy area (proxy set as  
227 0), while outside the sandy area, land degradation is more likely to happen in the absence of any policy  
228 effect (proxy set as 1, see Fig. S 2).

229 Table 1: Definition and derivation of drivers

Code	Name of driver	Definition of driver	Unit	Measures	Time series	Original format	Process approach	Data sources
Climate factors								
F1	temperature	Difference between average temperature / total precipitation in growth season (April-September) in Phase 1* and Phase 2*	°C	Mean temperature	2000, 2015- <del>2030</del>	Grid	Kriging via ArcGIS and Python language	National Meteorological Information Center ( <a href="https://data.cma.cn/">https://data.cma.cn/</a> )
F2	precipitation		mm	cumulative-rainfall	2000, 2015- <del>2030</del>			
Geographic factors								
F3	DEM	DEM	m	--		Grid	--	STRM
F4	slope	slope	degree	--		Grid	Reclassification	<a href="http://srtm.csi.cgiar.org/SELECTION/inputCoord.asp">http://srtm.csi.cgiar.org/SELECTION/inputCoord.asp</a>
F5	aspect	aspect	degree	--		Grid	Reclassification	
Distance measures								
F6	discrop	Change of distance to cropland in 2000 and 2015	m	Distance	2000, 2015	SHP	Euclidean	Extraction from land-use data
F7	disforest	Change of distance to forest in 2000 and 2015	m	Distance	2000, 2015			
F8	disunused	Change of distance to unused land 2000 and 2015	m	Distance	2000, 2015			
F9	disdense	Change of distance to dense grass 2000 and 2015	m	Distance	2000, 2015			
F10	dismode	Change of distance to moderate grass in 2000 and 2015	m	Distance	2000, 2015			
F11	dis sparse	Change of distance to sparse grass 2000 and 2015	m	Distance				
F12	disurban	Change of distance to urban in 2000 and 2015	m	Distance	2000, 2015			
F13	disrural	Change of distance to rural in 2000 and 2015	m	Distance	2000, 2015			



F1 4	disroad	Change of distance to road in 2000 and 2015	m	Distance	2000, 2015			
F1 5	dismine	Change of distance to mining in 2000 and 2015	m	Distance	2000, 2015			
F1 6	diswater	Change of distance to water in 2000 and 2015	m	Distance	2000, 2015			
Social-economic factors								
F1 7	population density	Change of population density in 2000 and 2010	Person	Person/ km2	2000, 2010	Grid	Density	Resource and Environment data cloud platform, CAS. ( <a href="http://www.resdc.cn/">http://www.resdc.cn/</a> )
F1 8	GDP*	Change of GDP in 2000 and 2010	Yuan	Yuan/km2	2000, 2010	Grid	Density	
F1 9	sheep density	Change of sheep density in 2000 and 2015	Sheep Unit	Sheep unit/km2	2000, 2015	Grid	Density	
Scenario setting								
F2 0	policy	--	--	(0,1)	--	Grid	--	Assumption

230 \*Note: Phase 1 refers to 1975-2000; Phase 2 refers to 2000-2015. GDP: gross  
231 domestic product.

### 232 2.3.1 XGBoost and logistic regression

233 Two algorithms were selected in this study: logistic regression (LR) and XGBoost. LR is a linear  
234 method involving two parts: the statistic LR and the classification LR. Both methods have already  
235 been used to simulate land use (Lin et al., 2011; Mustafa et al., 2018) and to define the relationship  
236 between land-use change and its drivers (~~Gollnow and Lakes, 2014; Mondal et al., 2014; Verburg et~~  
237 ~~al., 2002; Verburg and Chen, 2000~~)(Gollnow and Lakes, 2014; Mondal et al., 2014; Verburg et al.,  
238 2002; Verburg and Chen, 2000). Here, we use LR as a benchmark model to compare linear and non-  
239 linear methods in the simulation of land-use change. The optimised parameters of LG are  $C = 0.1$ ,  
240  $\text{penalty} = \text{l2}$ ,  $\text{solver} = \text{'lbfgs'}$ ,  $\text{multi\_class} = \text{'multinomial'}$ .

241 Boosting algorithms have been implemented in many past studies, where they often outperformed  
242 other ML algorithms (Ahmadlou et al., 2016; Filippi et al., 2014; Freeman et al., 2016; Keshtkar et  
243 al., 2017; Tayyebi and Pijanowski, 2014a). However, traditional boosting algorithms are often  
244 subject to overfitting (Georganos et al., 2018). To overcome this problem, Chen and Guestrin (2016)  
245 presented a new, regularised implementation of gradient boosting algorithms, which they called  
246 XGBoost (eXtreme Gradient Boosting). XGBoost was built as an enhanced version of the gradient  
247 boosting decision tree algorithm (GBDT), a regression and classification technique developed to  
248 predict results based on many weak prediction models – the decision tree (DT) (Abdullah et al.,  
249 2019; Freeman et al., 2016). XGBoost provides strong regularisation by adopting a stepwise  
250 shrinkage process instead of the traditional weighting process provided by GBDT. This process  
251 limits overfitting, minimises training losses and reduces classification errors while developing the  
252 final model (Abdullah et al., 2019; Hao Dong et al., 2018).

253 The XGBClassifier uses the following parameters:  $\text{learning\_rate}$  (controls learning itself);  
254  $\text{max\_depth}$  (control depth of the RF); the  $\text{n\_estimators}$  (controls the number of estimators used for  
255 the model); the  $\text{min\_child\_weight}$  (controls the complexity of a model, defines the minimum sum  
256 of weights of all observations required in a child); and  $\text{lambda}$  (L2 regularisation term on weights).  
257 The parameters were optimised using a simple grid search algorithm provided by scikit (Pedregosa  
258 et al., 2011) to estimate the optimal parameters ( $\text{learning\_rate} = 0.1$ ,  $\text{max\_depth} = 9$ ,  $\text{n\_estimator} =$   
259  $500$ ,  $\text{min\_child\_weight} = 3$ ,  $\text{lambda} = 10$ ).

### 260 2.3.2 Sampling methods

261 Data are often distributed unevenly among different classes (Vluymans, 2019). Such imbalanced  
262 class distribution generally induces a bias. Canonical ML algorithms assume that data is roughly  
263 balanced in different classes. In real situations, however, the data is usually skewed, and smaller  
264 classes often carry more important information and knowledge than larger ones (Krawczyk, 2016).  
265 It is therefore important to develop learning from imbalanced data to build real-world models  
266 (Krawczyk, 2016; Vluymans, 2019). To ensure a highly accurate GD model, we introduced four  
267 different sampling methods in this study (Fig. S 3).

268 **Balanced sampling:** Random data sampling, resulting in equal sized samples.

269 **Imbalanced sampling:** Random data sampling, but with the same share of the sampled class,  
270 resulting in unequal sized samples.

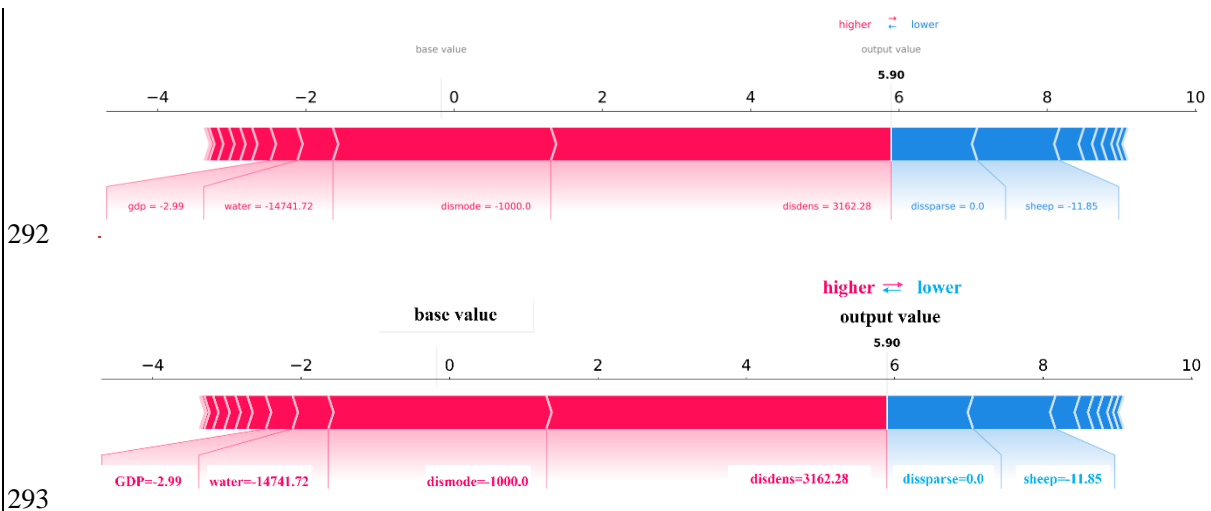
271 **Over-sampling:** Artificial points are added to the minority class of an imbalanced sampling set,  
272 making it equal to the majority class and resulting in equal sized samples.

273 **Under-sampling:** Points are removed from a majority class of an imbalanced sampling set,  
274 making it equal to the minority class and resulting in equal sized samples (He and Garcia, 2009).

275 In the present study, we used these four sampling methods to evaluate the model in the context of  
 276 the sampling method and its performance in the training process and the simulation process (see Fig.  
 277 S 3). In our case study, 18,190,000 pixels (about 10% of the total; including 18,190 pixels with  
 278 value 0 indicating no-change areas and restored grassland and 1,810 pixels with value 1 indicating  
 279 newly added grassland degradation) were selected by different sampling methods (Fig. S 3) to train  
 280 (66% of the sample size) and test (34% of the sample size) the model.

### 281 2.3.3 SHAP values

282 SHAP (SHapley Additive exPlanations) is a novel approach to improve our understanding of the  
 283 complexity of predictive model results and to explore relationships between individual variables for  
 284 the predicted case (Lundberg and Lee, 2017). SHAP is a useful method to sort the driver's effects,  
 285 and break down the prediction into individual feature impacts. Feature selection is of primary  
 286 concern when using ML methods to process land-use change (Samardžić-Petrović et al., 2015, 2016,  
 287 2017). SHAP values show the extent to which a given feature has changed the prediction, and allows  
 288 the model builder to decompose any prediction into the sum of the effects of each feature value and  
 289 explain – in our case – the predicted NGD probability for each pixel (see Figure 3). In this study,  
 290 we used SHAP values to sort the driver's attributions; capture the relationship between drivers and  
 291 NGD; and map the primary driver for NGD at the pixel level.



292  
 293  
 294 Figure 2: Decomposed SHAP values for the individual prediction of an example pixel.

295 In our study, we define the *base value* as the value that would be predicted by the model if no feature  
 296 knowledge were provided for the current output (mean prediction); we define the output value as  
 297 the prediction for this particular observation. SHAP values are calculated in log odds. Features that  
 298 increase the value of the prediction (to the left in Fig. 2) are always shown in red; those that lower  
 299 the prediction value are shown in blue (to the right in Fig. 2, Dataman, 2019). In this instance (Figure  
 300 2), *disdense* (change of distance to dense grass) is the primary driver of NGD at this pixel level  
 301 (largest value). The fact that the value is positive means that the risk of NDG increases in line with  
 302 an increase in distance to dense grass areas.

### 303 2.3.4 Validation of the model

304 Two validation steps are required for ML models: validation of the training process, and validation  
 305 of the simulation process. For the training process, a robust model was selected using overall  
 306 classification accuracy, precision, recall and the kappa index. Accuracy, precision and recall were

307 calculated based on a confusion matrix (CM) (He and Garcia, 2009). For the simulation process, the  
 308 final model was validated using the kappa index, the area under the precision-recall curve, and recall.  
 309 The validation indicators are defined as follows.

310 Overall classification accuracy (ACC) is the correct prediction of NGD and other pixels in the whole  
 311 region. This indicator was used to evaluate the accuracy of the model. Precision is the proportion of  
 312 correctly predicted positive examples (refers to NGD in this study) in all predicted positive examples.  
 313 Recall is the proportion of correctly predicted positive examples in all observed positive examples  
 314 (the observed NGD) (Sokolova and Lapalme, 2009). In general, high precision predictions have a  
 315 low recall, and vice versa, depending on the predicted goals. Here, since we focus on NGD and  
 316 other land-use changes, we use both indicators to evaluate our models.

317 Table 2: Confusion matrix for binary classification of newly added grassland degradation (NGD) and  
 318 other changes, including four indicators: false positives (FP), cells that were predicted as non-change but  
 319 changed in the observed map; false negatives (FN), cells that were predicted as change, but did not  
 320 change in the observed map for disagreement; true positives (TP), cells that were predicted as change  
 321 and changed in the observed map; and true negatives (TN), cells that were predicted as non-change and  
 322 did not change in the observed map for agreement.

Simulated values	Observed values			Recall=TP/ (TP+FN)
	Others NGD	Others True negatives (TN) False negatives (FN)	NGD False positives (FP) True positives (TP)	
		Precision =TP/(TP+FP)		
		ACC=(TP+TN)/(TP+FN+FP+TN)		

323 The precision-recall curve (PR curve) provides more information about the model's performance  
 324 than, for instance, the Receiver Operator Characteristic curve (ROC curve), when applied to skewed  
 325 data (Davis and Goadrich, 2006). The PR curve shows the trade-off of precision and recall, and  
 326 provides a model-wide evaluation. The area under the PR curve (AUC-PR) is likewise effective in  
 327 the classification of model comparisons. The baseline for the PR curve (y) is determined by positives  
 328 (P) and negatives (N). In our study,  $y = 0.09$  ( $y = 18374/200652$ ), which means when AUC-PR =  
 329 0.09, the model is a random model (Brownlee, 2018; Davis and Goadrich, 2006).

330 The kappa index ( $\kappa$ ) is a popular indicator used to measure the proportion of agreement between  
 331 observed and simulated data, especially to measure the degree of spatial matching. When  $\kappa > 0.8$ ,  
 332 strong agreement is yielded between the simulation and the observed map;  $0.6 < \kappa < 0.8$  describes  
 333 high agreement;  $0.4 < \kappa < 0.6$  describes moderate agreement; and  $\kappa < 0.4$  represents poor agreement  
 334 (Landis and Koch, 1977).

335 In this study,  $\kappa$  was used to evaluate the agreement and disagreement between observed NGD and  
 336 simulated NGD. Kappa should be the primary validation measure, followed by AUC-PR (used to  
 337 evaluate model performance) and recall (used to evaluate model sensitivity). Features and  
 338 definitions of these indicators are given below.

### 339 2.3.5 The structure of the ML model

340 The ML methodology of simulating GD involves six steps (Fig. S 4): (1) Target definition and data  
 341 collection and processing; the targets of this study are to build a robust ML model for simulating  
 342 NGD, as well as visualising these complex relationships between various variables and the dynamics  
 343 of GD. A total of 20 drivers (D) of GD were collected. All dynamic drivers were processed by GIS  
 344 into raster files and exported into ASCII files as final inputs for the ML model. (2) Data organisation:  
 345 the ML model simulates land-use change as a classification task (Samardžić-Petrović et al., 2015,

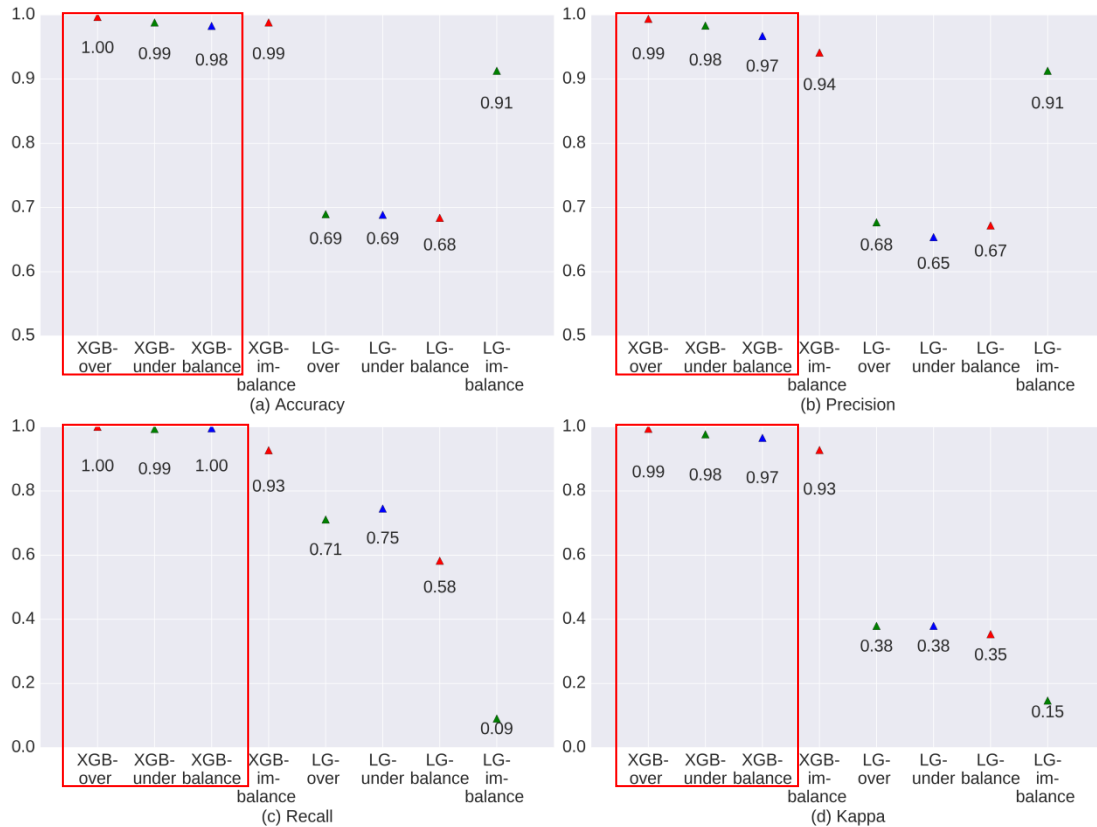
346 2017). In the present study, we organise this task as a binary classification  $Y$  (-value 1 and 0, stand  
347 for NGD and Non-NGD); related drivers are  $x$  ( $x_1, x_2, x_3, \dots, x_n$ ),  $n$  is the driver identifier, and  $x$   
348 denotes the change in value of each driver. The process of data standardisation is usually necessary  
349 for most ML models, but since XGBoost is a tree-based method, it does not require standardisation  
350 or normalisation. In this case, we performed standardisation only for the logistic regression model.  
351 (3) Data sampling: this is a necessary step to avoid overfitting or the loss of important information.  
352 The sampling method generally includes balanced and imbalanced sample strategies. In this study,  
353 we tested various balanced sampling strategies to identify the most suitable one. (4) Model building  
354 and selection: a ranking was used to find the best model in each specific case. In our study, we  
355 defined a model with  $\kappa > 0.8$  and  $AUC-PR > 0.09$  as robust, while  $0.6 < \kappa < 0.8$  and  $AUC-PR > 0.09$   
356 represents an acceptable model. (5) Model validation and feature ranking: after tuning the model,  
357 the most robust model and the driver with most useful information are selected. (6). The last step is  
358 explaining the model and the simulation. [The model used in training process was published in](#)  
359 [ZENODO \(Batunacun and Ralf Wieland, 2020\)](#)

## 360 **3. Results**

### 361 **3.1 Model validation**

362 The XGBoost model outperformed the LG model in both training and simulation (Figure 3 and 4).  
363 The LG model seems to be an inappropriate model for understanding NGD in this case. XGBoost  
364 yielded robust results in both training and simulation, with indicator values almost entirely above  
365 90%.

366 Figure 3 indicates that XGBoost performed very well across all balanced sampling methods (over-  
367 sampling, under-sampling and balanced sampling, red rectangle in Figure 3) in the training process.  
368 Only the imbalanced sampling exhibited a slightly weaker performance in the training process. This  
369 is mainly due to the balanced sampling datasets, which provided more information for the model.  
370 In addition, the model was affected less than the imbalanced sampling method by the majority class  
371 or unchanged cells (Mileva Samardzic-Petrovic et al., 2018).

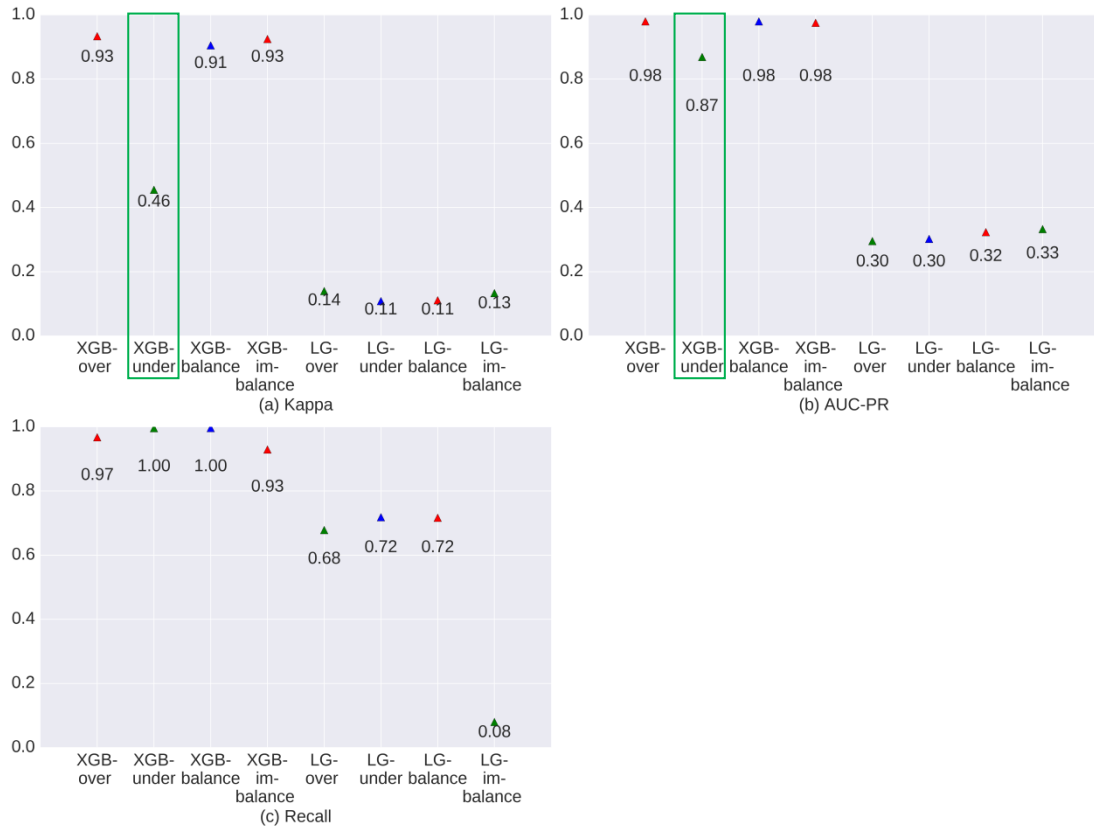


372

373 Figure 3: Evaluation of model performance during the training process for newly added grassland  
 374 between 1975–2015.

375 Figure 4 and Figure 5 show the model evaluation results in the simulation process and the spatial  
 376 prediction maps. XGBoost with under-sampling (green rectangle in Figure 4) yielded the weakest  
 377 performance compared to the other three sampling methods. This is mainly due to the smaller  
 378 sample size, which prevents the model from extracting sufficient experience. As can be seen in  
 379 Figure 5b, XGBoost used with the under-sampling method produced the error map with the highest  
 380 FP values, where the model predicted non-change points as change points. The under-sampling  
 381 method is unable to identify NGD points sufficiently well. XGBoost used with the over-sampling  
 382 method caused balanced and imbalanced sampling to have similar and strong prediction abilities  
 383 (see Figure 4), differing only slightly in their CM indicators (see Figure 5). We finally selected  
 384 XGBoost combined with the over-sampling strategy for our study, mainly because of its relatively  
 385 higher values in  $\kappa$ , AUC-PR and recall (see Figure 4).

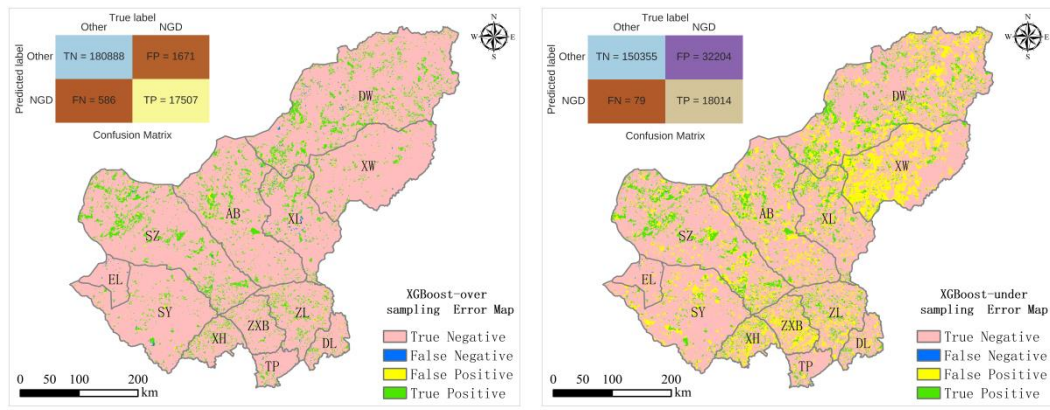
386



387

388  
389

Figure 4: Evaluation of model performance during the prediction process for newly added grassland between 1975–2015.

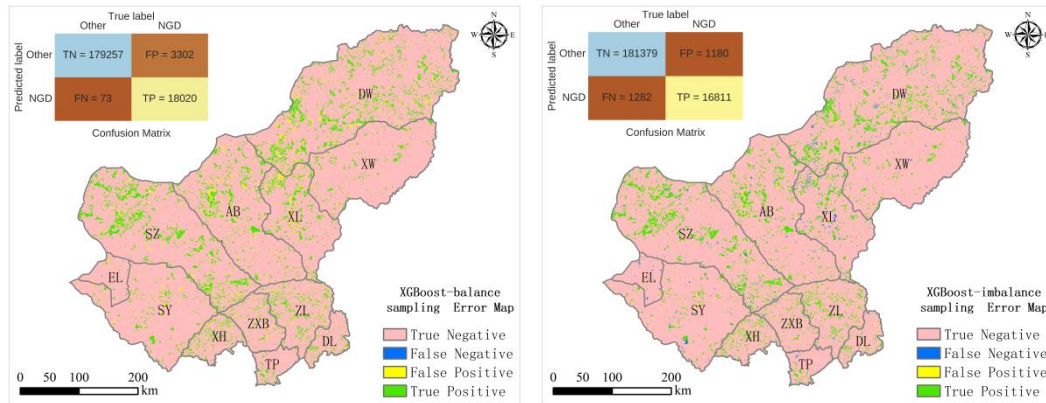


390

391

(a) Over-sampling

(b) Under-sampling



392

393

(c) Balanced sampling

(d) Imbalanced sampling

394

Figure 5: Error map of different sampling methods using the XGBoost model.

395

### 3.2 Driver selection

396

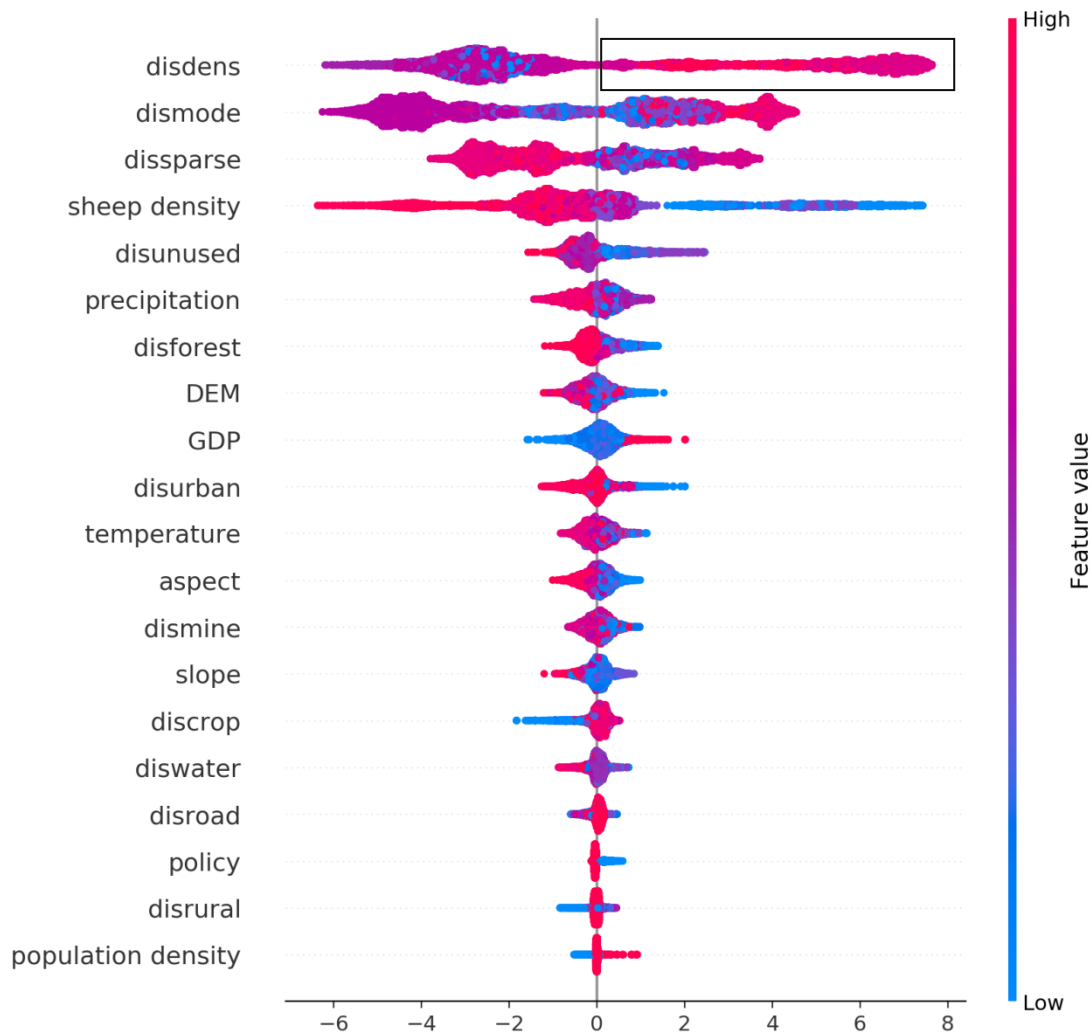
Figure 6 is a summary plot produced from the training dataset; it includes approximately 13,200 points (66% of the sample size). This plot combines feature importance (drivers are ordered along the y-axis) and driver effects (SHAP values on the x-axis), which describe the probability of NGD having occurred. Positive SHAP values refer to a higher probability of NGD. The gradient colour represents the feature value from high (red) to low (blue), as previously introduced in Figure 2. As Figure 6 shows, *disdense* was the primary driver for NGD in the study region. The relationship between *disdense* and NGD is non-linear, which can be seen from the SHAP values being both positive and negative (black rectangle in Figure 6). The interpretation of the effects of *disdense* can be summarised as a higher probability of NGD with increasing distance from dense grassland (see black rectangle in Figure 6 with pink colour on the right).

406

Figure 6 shows that driver effects include both linear-dominated relationships, such as *sheep*, *GDP* and others, and non-linear-dominated relations, such as *disdense*, *dismode* and others. In addition, the figure shows that the most important drivers for NGD are the changes of distance to dense, moderately dense and sparse grassland, then followed by sheep density and the distance to unused land. The effect of policies comes almost at the bottom, indicating that policies implemented outside sandy areas seem to have little effect on GD. The geographical factors DEM and slope are also positioned mid-field. The effect of geographical drivers does not appear to be as strong as the effect of other drivers. The change of distance to mining, located at the bottom for all drivers, does not have a strong effect on NGD compared to other drivers.

414





415

416 Figure 6: Driver ranking by SHAP values based on the training dataset (66% of sample size) using the  
 417 over-sampling method.

418 Note: The top rank indicates the most significant effects across all predictions. Each point in the cloud to  
 419 the left represents a row from the original dataset. The colour code denotes high (red) to low (blue) feature  
 420 values. Positive SHAP values represent a higher likelihood of NGD, while negative values indicate lower  
 421 likelihoods. The range across the SHAP value space indicates the degradation probability, expressed as  
 422 the logarithm of the odds.

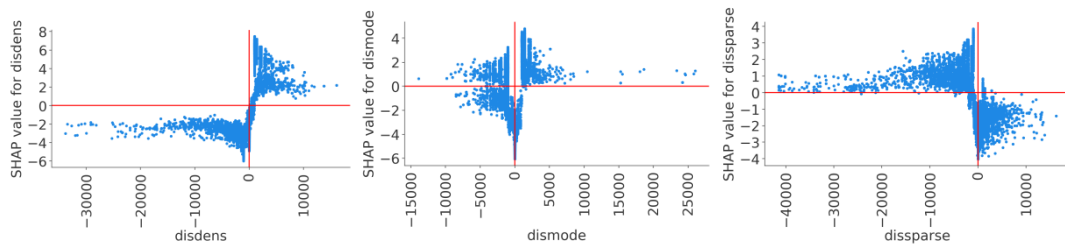
423 A recursive attribute elimination method was performed to determine how attribute reduction affects  
 424 modelling performance using XGBoost with the oversampling method (see Fig. S 5; for more details,  
 425 refer to Samardžić *et al.*, 2015). The results indicate that the first three drivers may already produce  
 426 a satisfactory model ( $\kappa = 0.74$ , AUC-PR = 0.85, recall = 0.92), while adding the fourth driver can  
 427 produce a robust model ( $\kappa = 0.94$ , AUC-PR = 0.98, recall = 0.98). This means that XGBoost used  
 428 with the oversampling strategy can predict NGD with very high accuracy using a relatively small  
 429 amount of data. Fig. S 6 shows the simulation result using the first four drivers, and compares the  
 430 results with the observed map.

### 431 3.3 Relationship between NGD and drivers in the XGBoost model

432 SHAP values and spread (Figure 7) indicate that no linear relationship between driver and prediction

433 could be found for any of the individual features. Change of distance to dense, moderately dense  
 434 and sparse grass pixels, and change of sheep density were the dominant drivers for NGD. Figure 7a  
 435 indicates that when  $disdense < 0$ , the SHAP value is negative, and when the distance to dense grass  
 436 areas is small, the likelihood of degradation is also small. The relationship seems to be more  
 437 complex for distance to moderately dense grass ( $dismode$ , Figure 7b); here, no simple linear  
 438 interpretation is obvious. For distance to sparse grass ( $dissparse$ , Figure 7c), the pattern again  
 439 suggests a rather linear interpretation, which is that the likelihood of degradation increases with  
 440 decreasing distance. For sheep density, Figure 7d indicates that when sheep density decreased, the  
 441 probability of GD obviously increased. Policy was not identified as a major driver of GD (Figure  
 442 6). However, policy effects obviously have a different impact inside and outside sandy zones. Figure  
 443 7e shows that our initial assumption is invalid: the probability of GD increased inside the sandy  
 444 areas where we assumed effective policy measures to be in place (value 0). This result is also in line  
 445 with Figure 7g, which shows that the closer to unused land, the more likely degradation will occur.

446 We can identify three groups for the remaining 14 drivers. For GDP and population density (Figure  
 447 7g and Figure 7h), the likelihood of NGD increases with increasing values. Figure 7i-j indicate that  
 448 warmer and drier climate conditions increase the probability of GD. Figure 7k, l, m and n indicate  
 449 that the probability of GD rises with closer distances to forest, urban, rural and water areas. Figure  
 450 7o shows a slight SHAP value pattern, in which the closer to cropland, the more unlikely degradation  
 451 will occur. This is mainly due to transformation from cropland to grassland. Figure 7p-t do not show  
 452 any interpretable spatial pattern.

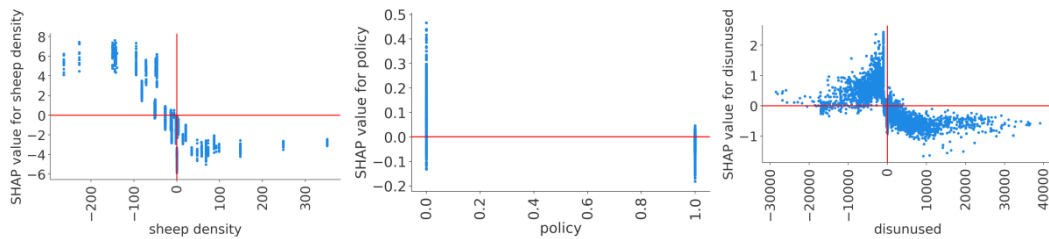


453

(a)

(b)

(c)

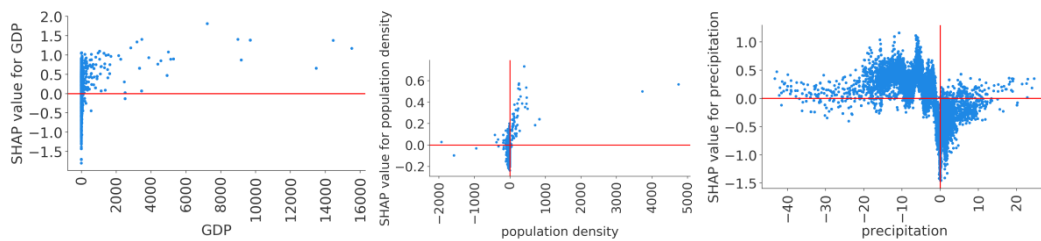


455

(d)

(e)

(f)



457

(g)

(h)

(i)

458

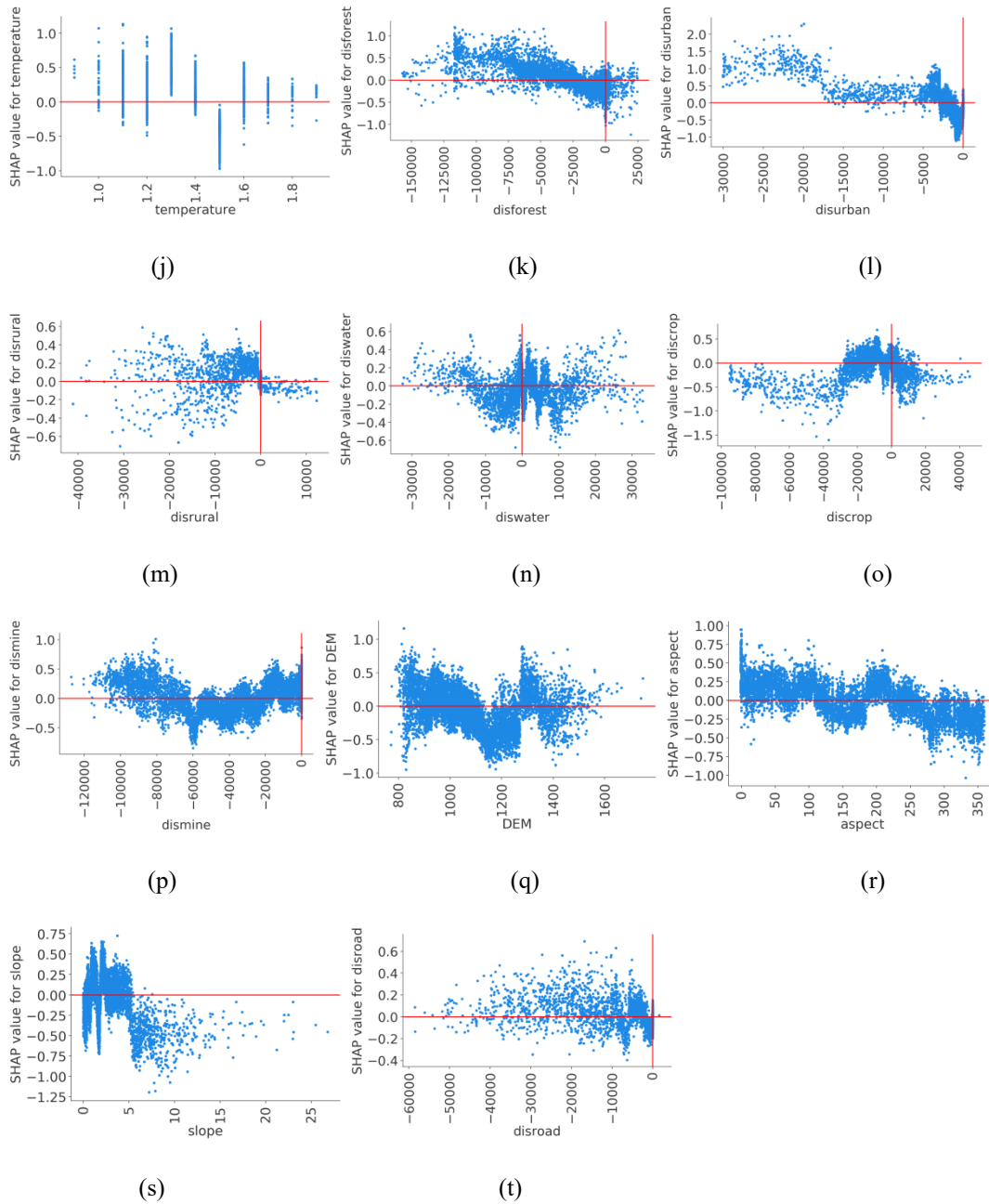
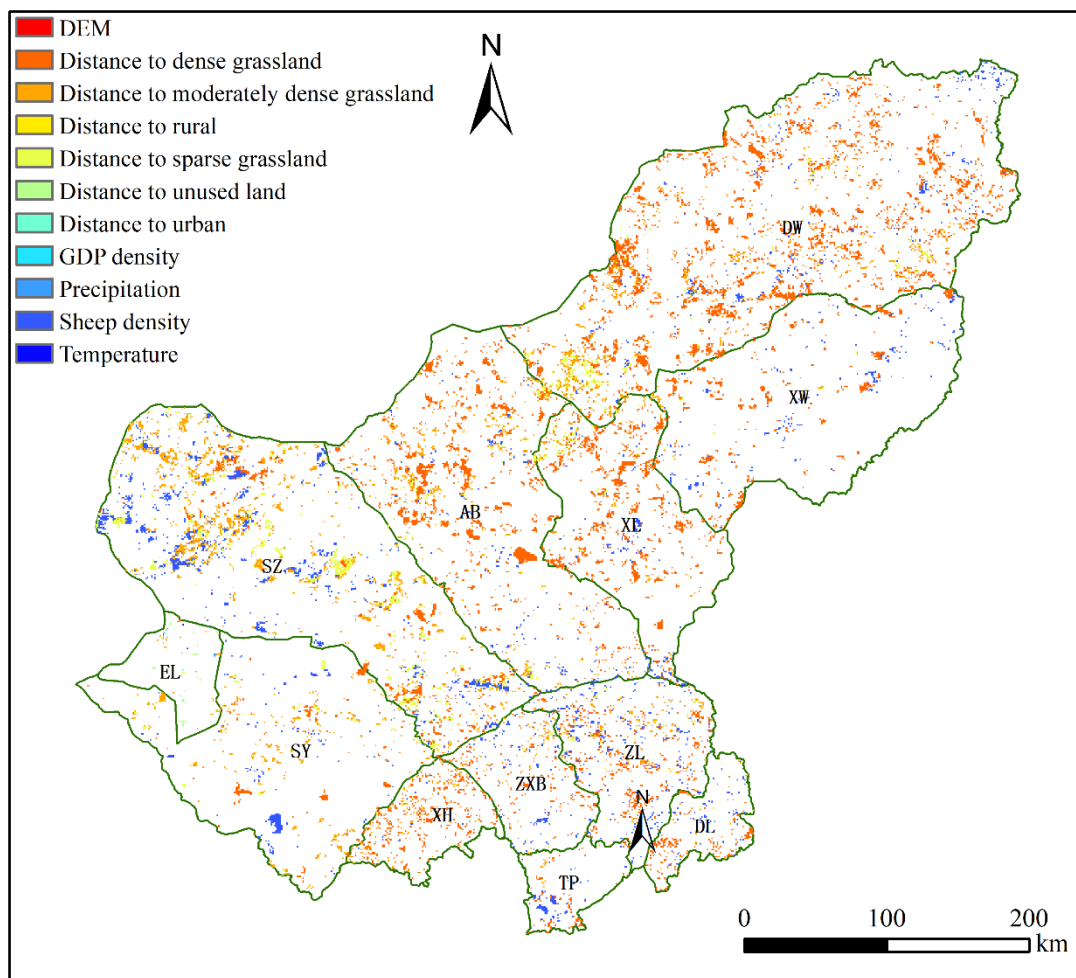


Figure 7: The SHAP dependence plot for each driver.

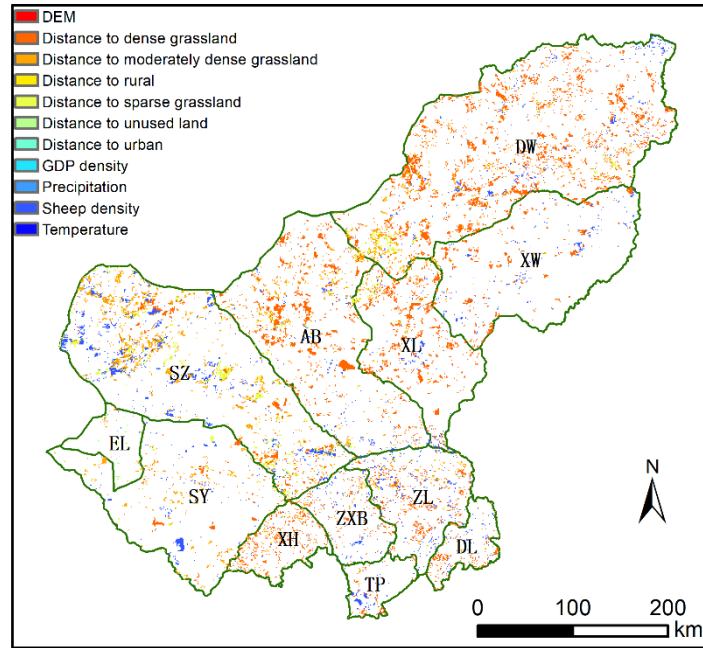
### 3.4 Mapping the primary drivers of NGD

All drivers' contributions to NGD were ranked according to their SHAP values for each pixel in this study. Figure 8 shows the primary driver for each NGD pixel. Distance to grassland pixels (dense, moderately dense and sparse grass) were the major drivers of NGD, responsible for 9,478, 3,892 and 1,629 NGD pixels, respectively. Sheep density was responsible for 3,042 NGD pixels, ranking third among all drivers. This order differs to that in Figure 6 and Figure 8 because in those cases, ranking is based on the total contribution of all drivers. Fig. S 7 shows the number of NGD pixels in which a driver was dominant or primary. The change of distance to any type of grassland was the primary driver for about 82.8% of the total NGD pixels; sheep density accounted for 16.8%. The

477 remaining seven drivers caused less than 1% of the total NGD. We can see from the spatial pattern  
478 that the change of distance to grassland was the major driver for GD in the dense grassland region  
479 (counties of DW, XL and AB), while in the counties of SZ, SY, ZXB, ZL and TP, sheep density was  
480 often identified as the major driver.



481



482

483

Figure 8: Spatial patterns of primary drivers for each pixel for NGD.

484

### 3.5 Regions of high risk for grassland degradation

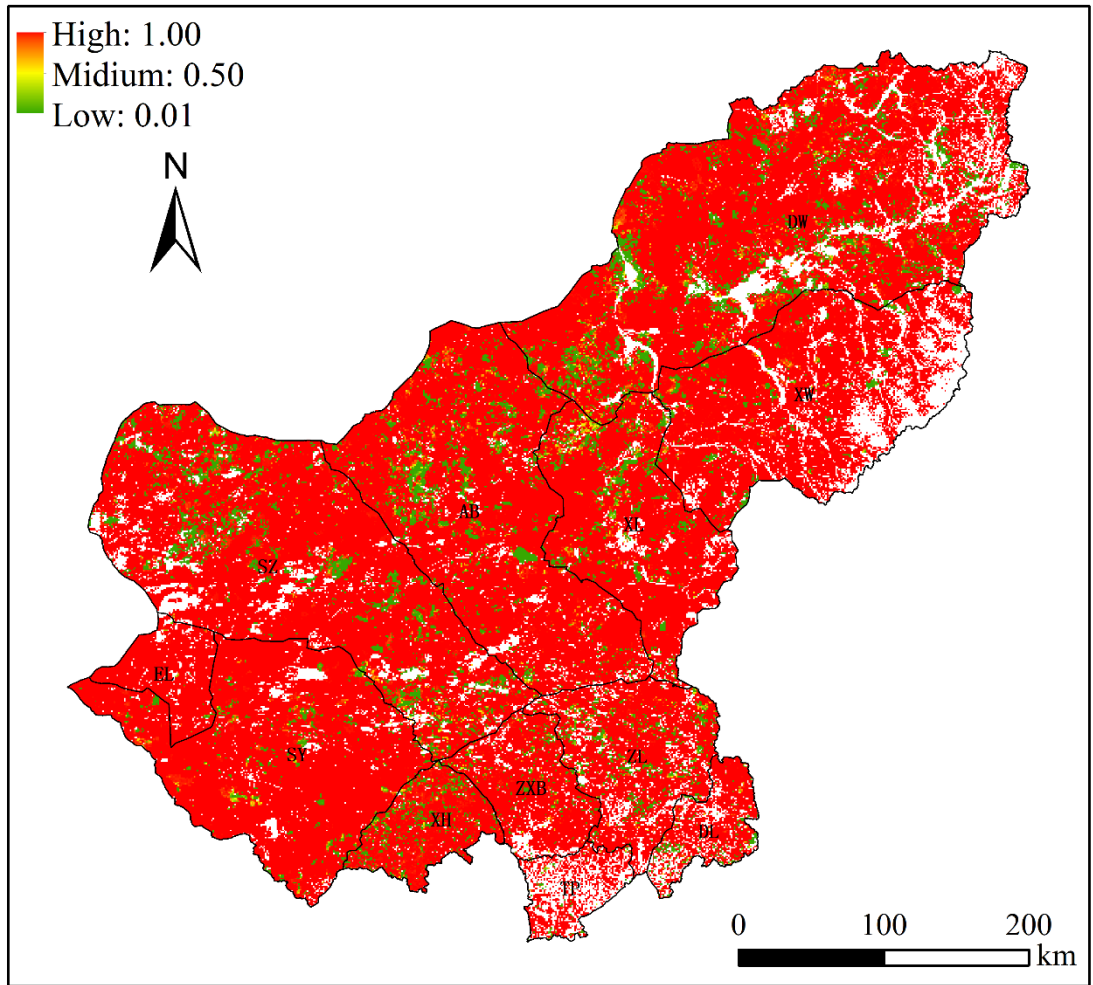
485

A probability map of NGD was produced (Figure 9). Low probabilities of NGD were found in the central and northern counties (DW, XL, AB, SZ, ZL ZXB and XH), while high probability regions were EL, SY and XW. TP and DL in the south were categorised as low probability regions, due to their lower share of grassland area.

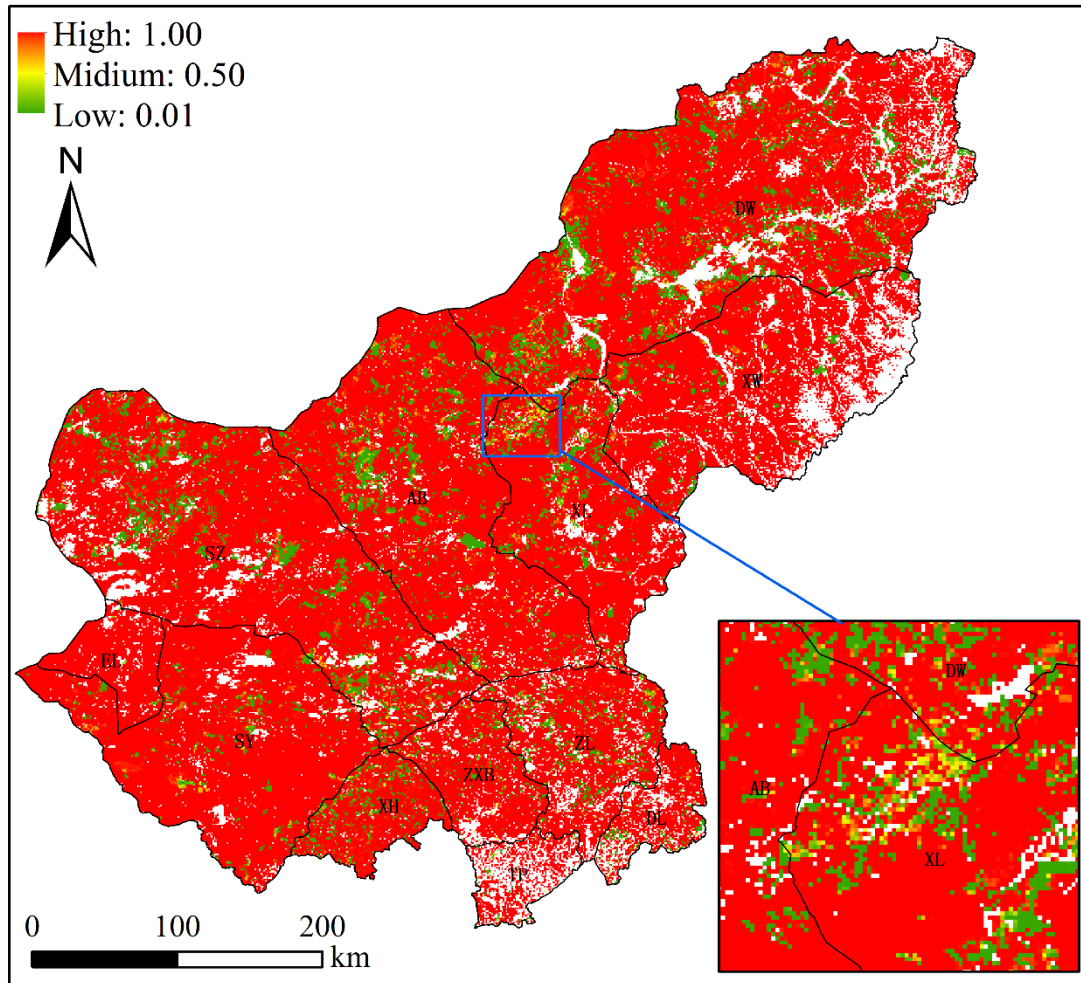
486

487

488



489



490

491 Figure 9: Degradation probability map for grassland in Xilingol, including a zoom into Xilinhot (XL)  
 492 for more details. The probability is based on the four most important drivers.

## 493 4. Discussion

### 494 4.1 ML model building and evaluation

495 In this study, we defined a general framework for creating an ML model using the XGBoost  
 496 algorithm for the purpose of analysing and predicting land-use change. XGBoost obtained a  $\kappa$  of  
 497 93% and a recall value of > 99% when used to simulate and predict GD in this study. Compared to  
 498 other popular ML learning algorithms, XGBoost exhibited a strong prediction ability. In studies  
 499 where ANN, SVM, RF, CART, Multivariate Adaptive Regression Spline (MARS) or LR were used  
 500 in combination with Cellular Automata (CA), the recall value is usually 54%-60% (Shafizadeh-  
 501 Moghadam et al., 2017). Ahmadi et al. (2019) stated that MARS and RF only yield high accuracy  
 502 in training runs, but do not prove very accurate in the validating process when simulating land-use  
 503 change.

504 Concerning the four sampling strategies we used to test the imbalance issue, we found that all  
 505 strategies performed satisfactorily in the training runs. In the simulation, the under-sampling  
 506 strategy yielded a relatively low accuracy ( $\kappa = 0.46$ ) model. We assume that removal of data from

507 the majority class causes the model to lose the important concepts pertaining to the majority class  
508 (He and Garcia, 2009). XGBoost used with the under-sampling method always produced similar  
509 results, irrespective of the size of the dataset (see Fig. S 8). We conclude from this pattern that  
510 XGBoost is also able to use sparse data to reflect real-world problems (Chen and Guestrin, 2016).

#### 511 4.2 SHAP values and drivers of grassland degradation

512 The general idea of introducing SHAP values as a further tool to analyse XGBoost ranking is to  
513 provide a method to evaluate the ranking with respect to causal relationships. The original XGBoost  
514 ranking is based on the in-built feature selection functions *Gain* (refers to the improvement in  
515 accuracy provided by a feature), *Weight* (or frequency, refers to the relative number of a feature  
516 occurrence in the trees of a model) and *Coverage* (refers to the relative numbers of observations  
517 related to this feature). However, these functions always produce different rankings of drivers (Abu-  
518 Rmoleh, 2019) due to random components in the algorithms. SHAP values introduce two further  
519 properties of feature importance measures: *consistency* (whenever we change a model such that it  
520 relies more on a feature, the attributed importance for that feature should not decrease) and *accuracy*  
521 (the sum of all feature importance values should equate to the total importance of the model;  
522 Lundberg, 2018; Lundberg & Lee, 2017). Consistency is required to stabilise the ranking throughout  
523 the analysis, reducing the change of order in the ranking to a minimum when the number of  
524 identified drivers changes. The accuracy property of SHAP makes sure that each driver's  
525 contribution to overall accuracy remains the same, even when drivers are excluded from analysis.  
526 Other methods usually compensate for the withdrawal of a driver from the analysis, which makes  
527 the determination of a single driver's contribution difficult.

528 The feature ranking based on SHAP values indicated that the change of distance to any type of  
529 grassland (dense, moderately dense and sparse grass) is the most important driver for any newly  
530 added grassland degradation. In this context, dense and moderately dense grassland areas are more  
531 easily degraded than other land-use types, followed by sparse grass. These results are in line with  
532 previous studies (Li et al., 2012; Xie and Sha, 2012)(Li et al., 2012; Xie and Sha, 2012). Good-  
533 quality grassland is more likely to be degraded through increasing human disturbance. An  
534 explanation for this can be derived from local people's living strategies. People who live in good-  
535 quality grassland areas are more likely to use grassland for livestock production with higher animal  
536 densities, risking overgrazing. Furthermore, Li et al. (2012)(2012) indicated that good-quality  
537 grassland is more likely to be converted to other land-use types, such as cropland. In contrast, people  
538 who have lived in sparse grassland regions for centuries have long adapted to low productivity,  
539 reducing their livestock numbers accordingly. They have also developed strategies to cope with  
540 variability in weather conditions, e.g. by preparing and storing more fodder and forage.

541 Sheep density was identified as the fourth major driver. However, the SHAP values indicate that  
542 when sheep density decreases, the probability of grassland degradation increases. Overgrazing has  
543 been the dominant driver for grassland degradation on the Mongolian plateau before, which has  
544 changed the grassland ecosystem significantly towards lower grass coverage (Nkonya et al., 2016;  
545 Wang et al., 2017). However, there is recent evidence that this causal relationship has changed. It  
546 now appears that farmers increasingly select their livestock numbers according to the carrying  
547 capacity of the grazing land (Cao et al., 2013b; Tiscornia et al., 2019b)(Cao et al., 2013b; Tiscornia  
548 et al., 2019b). By passing the "Fencing Grassland and Moving Users" policy (FGMU), the Chinese  
549 government issued a law that regulates livestock numbers based on a previously calculated carrying  
550 capacity. This development has upturned the causal relationship between livestock numbers and  
551 NGD, reflected by the SHAP value pattern in Figure 6.

552 Besides the four main drivers, seven other drivers also occasionally appear as the main driver for  
553 some pixels (Figure 8). This highlights the fact that, at the local level, other drivers apart from the  
554 four drivers identified as being major can also play a significant role. For example, in the county of



555 EL, the remaining seven drivers were mainly responsible for NGD. EL has less NGD after 2000  
556 compared with other counties in Xilingol (Fig. S 1), and most of the EL area is covered by sparse  
557 grass. EL is the most frequented border control point to Mongolia, and is subject to intensive tourism.

558 In the sparse grassland and agro-pastoral regions (SZ, SY, ZXB, ZL and TP), sheep density was  
559 identified as the important driver. This indicates that, even though livestock numbers have decreased,  
560 grassland is still experiencing serious degradation in this region. Here we see additional potential  
561 for installing further grassland conservation measures, such as adjusting the livestock number to the  
562 grassland carrying capacity.

#### 563 **4.3 The current risk of grassland degradation in Xilingol**

564 Three regions of different risk classes were identified in the probability map of NGD (Fig. 9). The  
565 low-risk region (DW, XL, AB, SZ, ZL ZXB and XH) is dominated by good-quality grassland (dense  
566 and moderately dense grass). In recent decades, this region has suffered from increasing human  
567 disturbance, e.g. overgrazing and mining development. However, after 2000, grassland in this region  
568 has recovered, mainly as the result of ecological protection projects (Sun et al., 2017). Even though  
569 this region is predicted as being less exposed to the risk of land degradation in the future, attention  
570 is still required for the restoration process. The high-risk region includes the counties of EL, SY and  
571 XW. EL and SY are covered by a large share of low-quality grassland, which – due to its own  
572 fragility – is likely to be affected by extreme climate and human disturbance, more than, e.g. higher-  
573 quality grasslands. The recent change in grassland property rights and the establishment of  
574 ecological protection projects have also limited the mobility of nomadic herders throughout Xilingol.  
575 As a consequence, herders cannot easily change grazing spots if extreme weather occurs; they are  
576 then bound to have their cattle graze at the same spots, increasing the pressure on low-quality  
577 grasslands in particular (Qian, 2011). For a long time, fragile grassland remained in an equilibrium  
578 state with the extreme weather (frequent droughts, “dudz”) to which it was exposed, and with the  
579 nomadic livestock husbandry that the region’s inhabitants practised. However, when the property  
580 rights of grassland and livestock were changed from collective to private, the nomadic lifestyle was  
581 largely abandoned.

#### 582 **4.4 The limitations of XGBoost for scenario exploration**

583 XGBoost has already scored top in a range of algorithm competitions in the data scientists  
584 community (Kaggle, 2019) due to its high accuracy and speed (Chen and Guestrin, 2016). ML  
585 models extract patterns from data, without considering any existing expert knowledge, which is why  
586 they are increasingly used to identify non-linear relationships (Ahmadlou et al., 2016; Samardžić-  
587 Petrović et al., 2015; Tayyebi and Pijanowski, 2014b). However, ML models require specific data  
588 structures for each problem to which they are applied. In this study, we simulated grassland  
589 degradation in two different phases (1975-2000 and 2000-2015). All time series of driver data were  
590 organised as model inputs, while grassland degradation dynamics were organised as prediction  
591 targets. Although the model achieved high accuracy in predicting NGD in Phase 2, it was not  
592 possible to achieve acceptable results in simulating both Phase 1 and Phase 2 separately. Second,  
593 compared with conventional models, the XGBoost model cannot be easily transferred to other  
594 regions for the same research question. Models like CLUE-S and GeoSOS-FLUS have been widely  
595 used in different regions across the world (Fuchs et al., 2017; Liang et al., 2018a; Liu et al., 2017;  
596 Verburg et al., 2002). (Fuchs et al., 2017; Liang et al., 2018a; Liu et al., 2017; Verburg et al., 2002).  
597 When ML models are used in other regions, driver data must be collected and structures adapted.  
598 Thirdly, ML models always need to learn sufficiently before they are able to make predictions. This  
599 requires a sufficient amount of data covering historical periods or different land-use change patterns.

600 XGBoost alone is unable to project any scenarios of land-use change based on historical data.  
601 However, the methodology presented here can be applied to quantify alternative scenarios produced

602 using other approaches, such as conventional, rule-based models (Verburg et al., 2002) or cellular  
603 automata (Islam et al., 2018; Shafizadeh-Moghadam et al., 2017).

604

## 605 **5 Conclusion**

606 Machine learning and data-driven approaches are becoming more and more important in many  
607 research areas. The design and development of a practical land-use model requires both accuracy  
608 and predictability to predict future land-use change, a well-fitted model that reflects and monitors  
609 the real world (Ahmadlou et al., 2019). The method framework presented here for building an ML  
610 model and explaining the relationship between drivers and grassland degradation identified  
611 XGBoost as a robust data-driven model for this purpose. XGBoost showed higher accuracy in  
612 training and simulation compared to existing ML models. Combined with over-sampling, it slightly  
613 outperformed in the simulation process. The simulated map has a high agreement with the observed  
614 values ( $\kappa=93\%$ ).

615 We identified six basic steps that should be included in ML model building, and they are also similar  
616 for other research applications (Kiyohara et al., 2018, 2018; Kontokosta and Tull, 2017;  
617 Subramaniyan et al., 2018). However, different validation measures can be introduced in both the  
618 training process and the simulation process. In this study, we tested different evaluation measures  
619 to evaluate the ML model, e.g. a typical confusion matrix to evaluate the training process, AUC-PR  
620 to evaluate the goodness of the ML model, and the kappa index to measure the degree of matching  
621 between observed and simulated values. These validation indicators consider both the research  
622 object and data characteristics. For example, when the data size is unbalanced, AUC-PR is a better  
623 choice than AUC-ROC (Brownlee, 2018; Davis and Goadrich, 2006; Saito and Rehmsmeier, 2015).

624 SHAP was introduced in this context to provide a causal explanation of the patterns identified by  
625 the ML model. In our case, SHAP was used to explain how drivers contribute to grassland  
626 degradation processes at the pixel and regional level, despite their non-linear relationship.  
627 According to the analysis, the distance to dense, moderately dense, and sparse grass, and sheep  
628 density, were the most important drivers that caused new grassland degradation in this region. In  
629 addition, individual SHAP values of sheep density indicated that the causal relationship between  
630 grassland degradation and livestock pressure has changed over time: the increase in sheep density  
631 was not the major driver for NGD in Phase 2 of the land degradation trajectory. Instead, the decrease  
632 in the grazing capacity of grassland caused a decrease in livestock numbers. The primary driver map  
633 of NGD provided a more detailed picture of NGD drivers for each pixel, as an important support  
634 for grassland management in the Xilingol region. The individual SHAP values of each driver may  
635 be an important prerequisite for rule-based scenario-building in the future.

### 636 **Author contribution:**

637 ~~Batunaeun~~B prepared the manuscript with contribution from all co-authors. ~~B gathered~~ and  
638 ~~Batunaeun~~prepared the data, performed the ~~simulation~~. ~~Ralf Wieland~~ develops simulations, and  
639 ~~analysed the output~~. ~~RW~~ developed the model code. ~~TL and CN~~ developed the research questions  
640 ~~and the outline of the study~~.

### 641 **Code and data availability**

642 ~~The development of XGBoost and SHAP values, graphs and model validation presented in this~~  
643 ~~paper were conducted in Python language. The original source code for XGBoost was obtained from~~

644 ~~website (<https://xgboost.readthedocs.io/en/latest/>) and the explanation of XGBoost could be~~  
645 ~~obtained from Chen et al (2016). The original source code of SHAP values could be found in GitHub~~  
646 ~~(<https://github.com/slundberg/shap>), while the explanation could be obtained from Lundberg et al~~  
647 ~~(2017). The land use data in this manuscript can be downloaded Resource and Environment data~~  
648 ~~cloud platform, CAS (<http://www.resde.cn/>), the statistical data could be obtained from Inner~~  
649 ~~Mongolia statistic year book. Other data get from various data sources, please check Table 1.~~  
650 The development of XGBoost and SHAP values, graphs and model validation presented in this  
651 paper were conducted using Python. The python script and related data have been published at  
652 ZENODO (<https://zenodo.org/record/3937226#.Xw2M6egzZPY>).  
653 The used XGBoost algorithm including the SHAP library runs well on a modern (Intel or AMD) PC  
654 (4 cores or more, 16 GB RAM). The training and the simulation were made on Linux as operating  
655 system but should work also under Windows.

656

## 657 **Competing interests:**

658 The authors declare that they have no conflict of interest

## 659 **Acknowledgements**

660 The authors express their sincere thanks to the China Scholarship Council (CSC) for funding this  
661 research and to Elen Schofield for language editing.

662

663

## 664 **Reference**

665 Abdullah, A. Y. M., Masrur, A., Adnan, M. S. G., Baky, Md. A. A., Hassan, Q. K. and Dewan, A.:  
666 Spatio-temporal Patterns of Land Use/Land Cover Change in the Heterogeneous Coastal Region of  
667 Bangladesh between 1990 and 2017, *Remote Sens.*, 11(7), 790, doi:10.3390/rs11070790, 2019.

668 Abu-Rmileh, A.: Be careful when interpreting your features importance in XGBoost!, *Data Sci.*  
669 [online] Available from: [https://towardsdatascience.com/be-careful-when-interpreting-your-](https://towardsdatascience.com/be-careful-when-interpreting-your-features-importance-in-xgboost-6e16132588e7)  
670 [features-importance-in-xgboost-6e16132588e7](https://towardsdatascience.com/be-careful-when-interpreting-your-features-importance-in-xgboost-6e16132588e7) (Accessed 14 June 2019), 2019.

671 Ahmadlou, M., Delavar, M. R. and Tayyebi, A.: Comparing ANN and CART to Model Multiple  
672 Land Use Changes: A Case Study of Sari and Ghaem-Shahr Cities in Iran, *JGST*, 6(1), 12, 2016.

673 Ahmadlou, M., Delavar, M. R., Basiri, A. and Karimi, M.: A Comparative Study of Machine  
674 Learning Techniques to Simulate Land Use Changes, *J. Indian Soc. Remote Sens.*, 47(1), 53–62,  
675 doi:10.1007/s12524-018-0866-z, 2019.

676 Akiyama, T. and Kawamura, K.: Grassland degradation in China: Methods of monitoring,  
677 management and restoration, *Grassl. Sci.*, 53(1), 1–17, doi:10.1111/j.1744-697X.2007.00073.x,  
678 2007.

679 Allington, G. R. H., Fernandez-Gimenez, M. E., Chen, J. and Brown, D. G.: Combining  
680 participatory scenario planning and systems modeling to identify drivers of future sustainability on  
681 the Mongolian Plateau, *Ecol. Soc.*, 23(2), art9, doi:10.5751/ES-10034-230209, 2018.

- 682 Anon: Resources and Environment Data Cloud Platform, Chinese Academic Science, [online]  
683 Available from: <http://www.geodata.cn/> (Accessed 29 October 2018), 2018.
- 684 [Batunacun and Ralf Wieland: XGBoost-SHAP values, prediction of grassland degradation, Zenodo.,](#)  
685 [2020.](#)
- 686 Batunacun, Wieland, R., Lakes, T., Yunfeng, H. and Nendel, C.: Identifying drivers of land  
687 degradation in Xilingol, China, between 1975 and 2015, *Land Use Policy*, 83, 543–559,  
688 doi:10.1016/j.landusepol.2019.02.013, 2019.
- 689 Bengtsson, J., Bullock, J. M., Egoh, B., Everson, C., Everson, T., O'Connor, T., O'Farrell, P. J.,  
690 Smith, H. G. and Lindborg, R.: Grasslands-more important for ecosystem services than you might  
691 think, *Ecosphere*, 10(2), e02582, doi:10.1002/ecs2.2582, 2019.
- 692 Brownlee, J.: How and When to Use ROC Curves and Precision-Recall Curves for Classification in  
693 Python, *Mach. Learn. Mastery* [online] Available from: [https://machinelearningmastery.com/roc-](https://machinelearningmastery.com/roc-curves-and-precision-recall-curves-for-classification-in-python/)  
694 [curves-and-precision-recall-curves-for-classification-in-python/](https://machinelearningmastery.com/roc-curves-and-precision-recall-curves-for-classification-in-python/) (Accessed 19 July 2019), 2018.
- 695 Cao, J., Yeh, E. T., Holden, N. M., Qin, Y. and Ren, Z.: The Roles of Overgrazing, Climate Change  
696 and Policy As Drivers of Degradation of China's Grasslands, *Nomadic Peoples*, 17(2), 82–101,  
697 doi:10.3167/np.2013.170207, 2013a.
- 698 Cao, J., Yeh, E. T., Holden, N. M., Qin, Y. and Ren, Z.: The Roles of Overgrazing, Climate Change  
699 and Policy As Drivers of Degradation of China's Grasslands, *Nomadic Peoples*, 17(2), 82–101,  
700 doi:10.3167/np.2013.170207, 2013b.
- 701 [Cao, M., Zhu, Y., Quan, J., Zhou, S., Lü, G., Chen, M. and Huang, M.: Spatial Sequential Modeling](#)  
702 [and Predication of Global Land Use and Land Cover Changes by Integrating a Global Change](#)  
703 [Assessment Model and Cellular Automata, \*Earths Future\*, 7\(9\), 1102–1116,](#)  
704 [doi:10.1029/2019EF001228, 2019.](#)
- 705 [Charif, O., Omrani, H., Abdallah, F. and Pijanowski, B.: A multi-label cellular automata model for](#)  
706 [land change simulation, \*Trans. GIS\*, 21\(6\), 1298–1320, doi:10.1111/tgis.12279, 2017.](#)
- 707 Chen, T. and Guestrin, C.: XGBoost: A Scalable Tree Boosting System, in *Proceedings of the 22nd*  
708 *ACM SIGKDD International Conference on Knowledge Discovery and Data Mining - KDD '16*,  
709 pp. 785–794, ACM Press, San Francisco, California, USA., 2016.
- 710 Dataman: Explain Your Model with the SHAP Values - Towards Data Science, *Data Sci.* [online]  
711 Available from: [https://towardsdatascience.com/explain-your-model-with-the-shap-values-](https://towardsdatascience.com/explain-your-model-with-the-shap-values-bc36aac4de3d)  
712 [bc36aac4de3d](https://towardsdatascience.com/explain-your-model-with-the-shap-values-bc36aac4de3d) (Accessed 8 October 2019), 2019.
- 713 Davis, J. and Goadrich, M.: The relationship between Precision-Recall and ROC curves, in  
714 *Proceedings of the 23rd international conference on Machine learning - ICML '06*, pp. 233–240,  
715 ACM Press, Pittsburgh, Pennsylvania., 2006.
- 716 Feng, Y., Liu, Y., Tong, X., Liu, M. and Deng, S.: Modeling dynamic urban growth using cellular  
717 automata and particle swarm optimization rules, *Landsc. Urban Plan.*, 102(3), 188–196,  
718 doi:10.1016/j.landurbplan.2011.04.004, 2011.
- 719 Filippi, A. M., Güneralp, İ. and Randall, J.: Hyperspectral remote sensing of aboveground biomass  
720 on a river meander bend using multivariate adaptive regression splines and stochastic gradient  
721 boosting, *Remote Sens. Lett.*, 5(5), 432–441, doi:10.1080/2150704X.2014.915070, 2014.

- 722 Freeman, E. A., Moisen, G. G., Coulston, J. W. and Wilson, B. T.: Random forests and stochastic  
723 gradient boosting for predicting tree canopy cover: comparing tuning processes and model  
724 performance, *Can. J. For. Res.*, 46(3), 323–339, doi:10.1139/cjfr-2014-0562, 2016.
- 725 Fu, Q., Hou, Y., Wang, B., Bi, X., Li, B. and Zhang, X.: Scenario analysis of ecosystem service  
726 changes and interactions in a mountain-oasis-desert system: a case study in Altay Prefecture, China,  
727 *Sci. Rep.*, 8(1), doi:10.1038/s41598-018-31043-y, 2018.
- 728 Fuchs, R., Prestele, R. and Verburg, P. H.: A global assessment of gross and net land change  
729 dynamics for current conditions and future scenarios, *Earth Syst. Dyn. Discuss.*, 1–29,  
730 doi:10.5194/esd-2017-121, 2017.
- 731 Georganos, S., Grippa, T., Vanhuyse, S., Lennert, M., Shimoni, M. and Wolff, E.: Very High  
732 Resolution Object-Based Land Use–Land Cover Urban Classification Using Extreme Gradient  
733 Boosting, *IEEE Geosci. Remote Sens. Lett.*, 15(4), 607–611, doi:10.1109/LGRS.2018.2803259,  
734 2018.
- 735 Gollnow, F. and Lakes, T.: Policy change, land use, and agriculture: The case of soy production and  
736 cattle ranching in Brazil, 2001–2012, *Appl. Geogr.*, 55, 203–211, doi:10.1016/j.apgeog.2014.09.003,  
737 2014.
- 738 Hao Dong, Xin Xu, Lei Wang and Fangling Pu: Gaofen-3 PolSAR Image Classification via  
739 XGBoost and Polarimetric Spatial Information, *Sensors*, 18(2), 611, doi:10.3390/s18020611, 2018.
- 740 He, Shi, P., Li, X., Chen, J., Li, Y. and Li, J.: Developing Land Use Scenario Dynamics Model by  
741 the Integration of System Dynamics Model and Cellular Automata Model, , 4, 2004.
- 742 He, H. and Garcia, E. A.: Learning from Imbalanced Data, *IEEE Trans. Knowl. Data Eng.*, 21(9),  
743 1263–1284, doi:10.1109/TKDE.2008.239, 2009.
- 744 Hoffmann, C., Funk, R., Wieland, R., Li, Y. and Sommer, M.: Effects of grazing and topography on  
745 dust flux and deposition in the Xilingele grassland, Inner Mongolia, *J. Arid Environ.*, 72(5), 792–  
746 807, doi:10.1016/j.jaridenv.2007.09.004, 2008.
- 747 Huang, B., Xie, C., Tay, R. and Wu, B.: Land-Use-Change Modeling Using Unbalanced Support-  
748 Vector Machines, *Environ. Plan. B Plan. Des.*, 36(3), 398–416, doi:10.1068/b33047, 2009.
- 749 Huang, B., Xie, C. and Tay, R.: Support vector machines for urban growth modeling,  
750 *GeoInformatica*, 14(1), 83–99, doi:10.1007/s10707-009-0077-4, 2010.
- 751 Islam, K., Rahman, Md. F. and Jashimuddin, M.: Modeling land use change using Cellular Automata  
752 and Artificial Neural Network: The case of Chunati Wildlife Sanctuary, Bangladesh, *Ecol. Indic.*,  
753 88, 439–453, doi:10.1016/j.ecolind.2018.01.047, 2018.
- 754 Jacquin, A., Goulard, M., Hutchinson, J. M. S., Devienne, T. and Hutchinson, S. L.: A statistical  
755 approach for predicting grassland degradation in disturbance-driven landscapes, *J. Environ. Prot.*,  
756 7, 912–925, doi:10.4236/jep.2016.76081ff. fhal-01509642ff, 2016.
- 757 Kaggle: Kaggle: Your Home for Data Science, [online] Available from: <https://www.kaggle.com/>  
758 (Accessed 5 January 2020), 2019.
- 759 Keshtkar, H., Voigt, W. and Alizadeh, E.: Land-cover classification and analysis of change using  
760 machine-learning classifiers and multi-temporal remote sensing imagery, *Arab. J. Geosci.*, 10(6),  
761 154, doi:10.1007/s12517-017-2899-y, 2017.

- 762 Khoury, A. E.: Modeling Land-Use Changes in the South Nation Watershed using Dyna-CLUE,  
763 University of Ottawa, Ottawa, Canada. [online] Available from: <http://hdl.handle.net/10393/22902>,  
764 2012.
- 765 Kiyohara, S., Miyata, T., Tsuda, K. and Mizoguchi, T.: Data-driven approach for the prediction and  
766 interpretation of core-electron loss spectroscopy, *Sci. Rep.*, 8(1), 1–12, doi:10.1038/s41598-018-  
767 30994-6, 2018.
- 768 Kontokosta, C. E. and Tull, C.: A data-driven predictive model of city-scale energy use in buildings,  
769 *Appl. Energy*, 197, 303–317, doi:10.1016/j.apenergy.2017.04.005, 2017.
- 770 Krawczyk, B.: Learning from imbalanced data: open challenges and future directions, *Prog. Artif.*  
771 *Intell.*, 5(4), 221–232, doi:10.1007/s13748-016-0094-0, 2016.
- 772 Krüger, C. and Lakes, T.: Bayesian belief networks as a versatile method for assessing uncertainty  
773 in land-change modeling, *Int. J. Geogr. Inf. Sci.*, 29(1), 111–131,  
774 doi:10.1080/13658816.2014.949265, 2015.
- 775 Kwon, H.-Y., Nkonya, E., Johnson, T., Graw, V., Kato, E. and Kihui, E.: Global Estimates of the  
776 Impacts of Grassland Degradation on Livestock Productivity from 2001 to 2011, in *Economics of*  
777 *Land Degradation and Improvement – A Global Assessment for Sustainable Development*, edited  
778 by E. Nkonya, A. Mirzabaev, and J. von Braun, pp. 197–214, Springer International Publishing,  
779 Cham., 2016.
- 780 Lakes, T., Müller, D. and Krüger, C.: Cropland change in southern Romania: a comparison of  
781 logistic regressions and artificial neural networks, *Landsc. Ecol.*, 24(9), 1195–1206,  
782 doi:10.1007/s10980-009-9404-2, 2009.
- 783 Landis, J. R. and Koch, G. G.: The Measurement of Observer Agreement for Categorical Data,  
784 *Biometrics*, 33(1), 159, doi:10.2307/2529310, 1977.
- 785 Li, S., Verburg, P. H., Lv, S., Wu, J. and Li, X.: Spatial analysis of the driving factors of grassland  
786 degradation under conditions of climate change and intensive use in Inner Mongolia, China, *Reg.*  
787 *Environ. Change*, 12(3), 461–474, doi:10.1007/s10113-011-0264-3, 2012.
- 788 Li, X. and Yeh, A. G.-O.: Neural-network-based cellular automata for simulating multiple land use  
789 changes using GIS, *Int. J. Geogr. Inf. Sci.*, 16(4), 323–343, doi:10.1080/13658810210137004, 2002.
- 790 Li, X., Zhou, W. and Ouyang, Z.: Forty years of urban expansion in Beijing: What is the relative  
791 importance of physical, socioeconomic, and neighborhood factors?, *Appl. Geogr.*, 38, 1–10,  
792 doi:10.1016/j.apgeog.2012.11.004, 2013.
- 793 Li, X., Bai, Y., Wen, W., Wang, H., Li, R., Li, G. and Wang, H.: Effects of grassland degradation  
794 and precipitation on carbon storage distributions in a semi-arid temperate grassland of Inner  
795 Mongolia, China, *Acta Oecologica*, 85, 44–52, doi:10.1016/j.actao.2017.09.008, 2017.
- 796 Liang, X., Liu, X., Li, X., Chen, Y., Tian, H. and Yao, Y.: Delineating multi-scenario urban growth  
797 boundaries with a CA-based FLUS model and morphological method, *Landsc. Urban Plan.*, 177,  
798 47–63, doi:10.1016/j.landurbplan.2018.04.016, 2018a.
- 799 Liang, X., Liu, X., Li, D., Zhao, H. and Chen, G.: Urban growth simulation by incorporating  
800 planning policies into a CA-based future land-use simulation model, *Int. J. Geogr. Inf. Sci.*, 32(11),  
801 2294–2316, doi:10.1080/13658816.2018.1502441, 2018b.

- 802 Lin, Y., Deng, X., Li, X. and Ma, E.: Comparison of multinomial logistic regression and logistic  
803 regression: which is more efficient in allocating land use?, *Front. Earth Sci.*, 8(4), 512–523,  
804 doi:10.1007/s11707-014-0426-y, 2014.
- 805 Lin, Y.-P., Chu, H.-J., Wu, C.-F. and Verburg, P. H.: Predictive ability of logistic regression, auto-  
806 logistic regression and neural network models in empirical land-use change modeling – a case study,  
807 *Int. J. Geogr. Inf. Sci.*, 25(1), 65–87, doi:10.1080/13658811003752332, 2011.
- 808 Liu, M., Dries, L., Heijman, W., Zhu, X., Deng, X. and Huang, J.: Land tenure reform and grassland  
809 degradation in Inner Mongolia, China, *China Econ. Rev.*, 55, 181–198,  
810 doi:10.1016/j.chieco.2019.04.006, 2019.
- 811 Liu, X., Liang, X., Li, X., Xu, X., Ou, J., Chen, Y., Li, S., Wang, S. and Pei, F.: A future land use  
812 simulation model (FLUS) for simulating multiple land use scenarios by coupling human and natural  
813 effects, *Landsc. Urban Plan.*, 168, 94–116, doi:10.1016/j.landurbplan.2017.09.019, 2017.
- 814 Lundberg, S. M. and Lee, S.-I.: *A Unified Approach to Interpreting Model Predictions*, pp. 4768–  
815 4777, Long Beach, California, USA., 2017.
- 816 Mileva Samardzic-Petrovic, Branislav Bajat, Miloš Kovačević and Suzana Dragicevic: Modelling  
817 and analysing land use changes with data-driven models: a review of application on the Belgrade  
818 study area, in *ResearchGate, Belgrade*. [online] Available from:  
819 [https://www.researchgate.net/publication/330910156\\_Modelling\\_and\\_analysing\\_land\\_use\\_changes\\_with\\_data-driven\\_models\\_a\\_review\\_of\\_application\\_on\\_the\\_Belgrade\\_study\\_area](https://www.researchgate.net/publication/330910156_Modelling_and_analysing_land_use_changes_with_data-driven_models_a_review_of_application_on_the_Belgrade_study_area) (Accessed 10  
820 March 2019), 2018.
- 822 Mondal, I., Srivastava, V. K., Roy, P. S. and Talukdar, G.: Using logit model to identify the drivers  
823 of landuse landcover change in the lower gangetic basin, india, *ISPRS - Int. Arch. Photogramm.*  
824 *Remote Sens. Spat. Inf. Sci.*, XL–8, 853–859, doi:10.5194/isprsarchives-XL-8-853-2014, 2014.
- 825 Mustafa, A., [Cools, M., Saadi, I. and Teller, J.: Coupling agent-based, cellular automata and logistic](#)  
826 [regression into a hybrid urban expansion model \(HUEM\), \*Land Use Policy\*, 69, 529–540,](#)  
827 [doi:10.1016/j.landusepol.2017.10.009, 2017.](#)
- 828 [Mustafa, A.,](#) Rienow, A., Saadi, I., Cools, M. and Teller, J.: Comparing support vector machines  
829 with logistic regression for calibrating cellular automata land use change models, *Eur. J. Remote*  
830 *Sens.*, 51(1), 391–401, doi:10.1080/22797254.2018.1442179, 2018.
- 831 National Research Council, N. R. C.: *Advancing Land Change Modeling: Opportunities and*  
832 *Research Requirements*, National Academies Press, Washington, D.C., 2014.
- 833 Nkonya, E., Mirzabaev, A. and von Braun, J., Eds.: *Economics of Land Degradation and*  
834 *Improvement – A Global Assessment for Sustainable Development*, Springer International  
835 Publishing, Cham., 2016.
- 836 Pedregosa, F., Varoquaux, G., Gramfort, A., Michel, V., Thirion, B., Grisel, O., Blondel, M.,  
837 Prettenhofer, P., Weiss, R., Dubourg, V., Vanderplas, J., Passos, A. and Cournapeau, D.: *Scikit-learn:*  
838 *Machine Learning in Python*, *Mach. Learn. PYTHON*, 12, 2825–2830, 2011.
- 839 Pijanowski, B. C., Brown, D. G., Shellito, B. A. and Manik, G. A.: Using neural networks and GIS  
840 to forecast land use changes: a Land Transformation Model, *Comput. Environ. Urban Syst.*, 26(6),  
841 553–575, doi:10.1016/S0198-9715(01)00015-1, 2002.
- 842 Pijanowski, B. C., Pithadia, S., Shellito, B. A. and Alexandridis, K.: Calibrating a neural network-

- 843 based urban change model for two metropolitan areas of the Upper Midwest of the United States,  
844 *Int. J. Geogr. Inf. Sci.*, 19(2), 197–215, doi:10.1080/13658810410001713416, 2005.
- 845 Qian, Z.: Herders' Social Vulnerability to Climate Change: A case of desert grassland in Inner  
846 Mongolia (in Chinese), *Sociol. Study*, (6), 171–195, 2011.
- 847 Reiche, M.: Wind erosion and dust deposition – A landscape in Inner Mongolia Grassland, China,  
848 Universität Potsdam, Germany., 2014.
- 849 Ren, Y., Lü, Y., Comber, A., Fu, B., Harris, P. and Wu, L.: Spatially explicit simulation of land  
850 use/land cover changes: Current coverage and future prospects, *Earth-Sci. Rev.*, 190, 398–415,  
851 doi:10.1016/j.earscirev.2019.01.001, 2019.
- 852 Saito, T. and Rehmsmeier, M.: The Precision-Recall Plot Is More Informative than the ROC Plot  
853 When Evaluating Binary Classifiers on Imbalanced Datasets, edited by G. Brock, *PLOS ONE*, 10(3),  
854 e0118432, doi:10.1371/journal.pone.0118432, 2015.
- 855 Samardžić-Petrović, M., Dragičević, S., Bajat, B. and Kovačević, M.: Exploring the Decision Tree  
856 Method for Modelling Urban Land Use Change, *GEOMATICA*, 69(3), 313–325,  
857 doi:10.5623/cig2015-305, 2015.
- 858 Samardžić-Petrović, M., Dragičević, S., Kovačević, M. and Bajat, B.: Modeling Urban Land Use  
859 Changes Using Support Vector Machines: Modeling Urban Land Use Changes Using Support  
860 Vector Machines, *Trans. GIS*, 20(5), 718–734, doi:10.1111/tgis.12174, 2016.
- 861 Samardžić-Petrović, M., Kovačević, M., Bajat, B. and Dragičević, S.: Machine Learning Techniques  
862 for Modelling Short Term Land-Use Change, *ISPRS Int. J. Geo-Inf.*, 6(12), 387,  
863 doi:10.3390/ijgi6120387, 2017.
- 864 Samie, A., Deng, X., Jia, S. and Chen, D.: Scenario-Based Simulation on Dynamics of Land-Use-  
865 Land-Cover Change in Punjab Province, Pakistan, *Sustainability*, 9(8), 1285,  
866 doi:10.3390/su9081285, 2017.
- 867 Shafizadeh-Moghadam, H., Asghari, A., Tayyebi, A. and Taleai, M.: Coupling machine learning,  
868 tree-based and statistical models with cellular automata to simulate urban growth, *Comput. Environ.  
869 Urban Syst.*, 64, 297–308, doi:10.1016/j.compenvurbsys.2017.04.002, 2017.
- 870 Shao, L., Chen, H., Zhang, C. and Huo, X.: Effects of Major Grassland Conservation Programs  
871 Implemented in Inner Mongolia since 2000 on Vegetation Restoration and Natural and  
872 Anthropogenic Disturbances to Their Success, *Sustainability*, 9(3), 466, doi:10.3390/su9030466,  
873 2017.
- 874 Sokolova, M. and Lapalme, G.: A systematic analysis of performance measures for classification  
875 tasks, *Inf. Process. Manag.*, 45(4), 427–437, doi:10.1016/j.ipm.2009.03.002, 2009.
- 876 Su, H., Liu, W., Xu, H., Wang, Z., Zhang, H., Hu, H. and Li, Y.: Long-term livestock exclusion  
877 facilitates native woody plant encroachment in a sandy semiarid rangeland, *Ecol. Evol.*, 5(12),  
878 2445–2456, doi:10.1002/ece3.1531, 2015.
- 879 Subramaniyan, M., Skoogh, A., Salomonsson, H., Bangalore, P. and Bokrantz, J.: A data-driven  
880 algorithm to predict throughput bottlenecks in a production system based on active periods of the  
881 machines, *Comput. Ind. Eng.*, 125, 533–544, doi:10.1016/j.cie.2018.04.024, 2018.
- 882 Sun, B., Li, Z., Gao, Z., Guo, Z., Wang, B., Hu, X. and Bai, L.: Grassland degradation and restoration



- 883 monitoring and driving forces analysis based on long time-series remote sensing data in Xilin Gol  
884 League, *Acta Ecol. Sin.*, 37(4), 219–228, doi:10.1016/j.chnaes.2017.02.009, 2017.
- 885 Sun, Z. and Müller, D.: A framework for modeling payments for ecosystem services with agent-  
886 based models, Bayesian belief networks and opinion dynamics models, *Environ. Model. Softw.*, 45,  
887 15–28, doi:10.1016/j.envsoft.2012.06.007, 2013.
- 888 Tayyebi, A. and Pijanowski, B. C.: Modeling multiple land use changes using ANN, CART and  
889 MARS: Comparing tradeoffs in goodness of fit and explanatory power of data mining tools, *Int. J.*  
890 *Appl. Earth Obs. Geoinformation, Complete*(28), 102–116, doi:10.1016/j.jag.2013.11.008, 2014a.
- 891 Tayyebi, A. and Pijanowski, B. C.: Modeling multiple land use changes using ANN, CART and  
892 MARS: Comparing tradeoffs in goodness of fit and explanatory power of data mining tools, *Int. J.*  
893 *Appl. Earth Obs. Geoinformation*, 28, 102–116, doi:10.1016/j.jag.2013.11.008, 2014b.
- 894 Tiscornia, G., Jaurena, M. and Baethgen, W.: Drivers, Process, and Consequences of Native  
895 Grassland Degradation: Insights from a Literature Review and a Survey in Río de la Plata Grasslands,  
896 *Agronomy*, 9(5), 239, doi:10.3390/agronomy9050239, 2019a.
- 897 Tiscornia, G., Jaurena, M. and Baethgen, W.: Drivers, Process, and Consequences of Native  
898 Grassland Degradation: Insights from a Literature Review and a Survey in Río de la Plata Grasslands,  
899 *Agronomy*, 9(5), 239, doi:10.3390/agronomy9050239, 2019b.
- 900 Tong, S., Bao, Y., Te, R., Ma, Q., Ha, S. and Lusi, A.: Analysis of Drought Characteristics in Xilingol  
901 Grassland of Northern China Based on SPEI and Its Impact on Vegetation, *Math. Probl. Eng.*, 2017,  
902 1–11, doi:10.1155/2017/5209173, 2017.
- 903 [Troost, C., Walter, T. and Berger, T.: Climate, energy and environmental policies in agriculture:  
904 Simulating likely farmer responses in Southwest Germany, \*Land Use Policy\*, 46, 50–64,  
905 doi:10.1016/j.landusepol.2015.01.028, 2015.](#)
- 906 Verburg, P. H. and Chen, Y.: Multiscale Characterization of Land-Use Patterns in China, *Ecosystems*,  
907 3(4), 369–385, doi:10.1007/s100210000033, 2000.
- 908 Verburg, P. H. and Veldkamp, A.: Projecting land use transitions at forest fringes in the Philippines  
909 at two spatial scales, *Landsc. Ecol.*, 19(1), 77–98, doi:10.1023/B:LAND.0000018370.57457.58,  
910 2004.
- 911 Verburg, P. H., Soepboer, W., Veldkamp, A., Limpiada, R., Espaldon, V. and Mastura, S. S. A.:  
912 Modeling the Spatial Dynamics of Regional Land Use: The CLUE-S Model, *Environ. Manage.*,  
913 30(3), 391–405, doi:10.1007/s00267-002-2630-x, 2002.
- 914 [Vermeiren, K., Vanmaercke, M., Beckers, J. and Van Rompaey, A.: ASSURE: a model for the  
915 simulation of urban expansion and intra-urban social segregation, \*Int. J. Geogr. Inf. Sci.\*, 30\(12\),  
916 2377–2400, doi:10.1080/13658816.2016.1177641, 2016.](#)
- 917 Vluymans, S.: Learning from Imbalanced Data, in *Dealing with Imbalanced and Weakly Labelled  
918 Data in Machine Learning using Fuzzy and Rough Set Methods*, vol. 807, pp. 81–110, Springer  
919 International Publishing, Cham., 2019.
- 920 Wang, X., Dong, S., Yang, B., Li, Y. and Su, X.: The effects of grassland degradation on plant  
921 diversity, primary productivity, and soil fertility in the alpine region of Asia's headwaters, *Environ.*  
922 *Monit. Assess.*, 186(10), 6903–6917, doi:10.1007/s10661-014-3898-z, 2014.

- 923 Wang, Y., Wang, Z., Li, R., Meng, X., Ju, X., Zhao, Y. and Sha, Z.: Comparison of Modeling  
 924 Grassland Degradation with and without Considering Localized Spatial Associations in Vegetation  
 925 Changing Patterns, *Sustainability*, 10(2), 316, doi:10.3390/su10020316, 2018.
- 926 Wang, Z., Deng, X., Song, W., Li, Z. and Chen, J.: What is the main cause of grassland degradation?  
 927 A case study of grassland ecosystem service in the middle-south Inner Mongolia, *CATENA*, 150,  
 928 100–107, doi:10.1016/j.catena.2016.11.014, 2017.
- 929 Xie, Y. and Sha, Z.: Quantitative Analysis of Driving Factors of Grassland Degradation: A Case  
 930 Study in Xilin River Basin, Inner Mongolia, *Sci. World J.*, 2012, 1–14, doi:10.1100/2012/169724,  
 931 2012.
- 932 Xu GC, Kang MY, Marc Metzger and Y Jiang: Vulnerability of the Human-Environment System in  
 933 Arid Regions: The Case of Xilingol Grassland in Northern China, *Pol. J. Environ. Stud.*, 23(5),  
 934 1773–1785, 2014.
- 935 [Yang, J., Chen, F., Xi, J., Xie, P. and Li, C.: A Multitarget Land Use Change Simulation Model  
 936 Based on Cellular Automata and Its Application, \*Abstr. Appl. Anal.\*, 2014, 1–11,  
 937 doi:10.1155/2014/375389, 2014.](#)
- 938 [Yang, X., Chen, R. and Zheng, X. Q.: Simulating land use change by integrating ANN-CA model  
 939 and landscape pattern indices, \*Geomat. Nat. Hazards Risk\*, 7\(3\), 918–932,  
 940 doi:10.1080/19475705.2014.1001797, 2016.](#)
- 941 Zhan J Y, Xiangzheng Deng, Ou Jiang and Nana Shi: The Application of System Dynamics and  
 942 CLUE-S Model in Land Use Change Dynamic Simulation: a Case Study in Taips County, Inner  
 943 Mongolia of China, in *Management Science*, pp. 2781–2790, Shanghai. [online] Available from:  
 944 [https://www.researchgate.net/publication/228986766\\_The\\_Application\\_of\\_System\\_Dynamics\\_and  
 945 CLUE-  
 946 S\\_Model\\_in\\_Land\\_Use\\_Change\\_Dynamic\\_Simulation\\_a\\_Case\\_Study\\_in\\_Taips\\_County\\_Inner\\_  
 947 Mongolia\\_of\\_China](https://www.researchgate.net/publication/228986766_The_Application_of_System_Dynamics_and_CLUE-S_Model_in_Land_Use_Change_Dynamic_Simulation_a_Case_Study_in_Taips_County_Inner_Mongolia_of_China) (Accessed 29 April 2018), 2007.
- 948 Zhang, M., Zhao, J. and Yuan, L.: Simulation of Land-Use Policies on Spatial Layout with the  
 949 CLUE-S Model, *ISPRS - Int. Arch. Photogramm. Remote Sens. Spat. Inf. Sci.*, XL-2/W1, 185–190,  
 950 doi:10.5194/isprsarchives-XL-2-W1-185-2013, 2013.
- 951
- 952